COLLISION BROADENING OF MICROWAVE SPECTRAL LINES OF MONOMERIC FORMALDEHYDE AND FORMIC ACID

DISSERTATION

Presented to the Graduate Council of the
North Texas State University in Partial
Fulfillment of the Requirements

For the Degree of

DOCTOR OF PHILOSOPHY

By

Arun C. Venkatachar, B.S., M.S.
Denton, Texas
August, 1975

Venkatachar, Arun C., Collision Broadening of Microwave Spectral Lines of Monomeric Formaldehyde and Formic Acid. Doctor of Philosophy (Physics), August, 1975, 105 pp., 6 tables, 26 illustrations, bibliography, 71 titles.

Line width parameters for a number of spectral lines in the pure rotational spectrum of formaldehyde (CH_2O) and formic acid (HCOOH) have been measured using a source-modulated microwave spectrograph. All transitions studied in this investigation were of the type $\Delta J=0$ (i.e. Q-branch transitions), with $\Delta K_{-1}=0$ and $\Delta K_{+1}=+1$. The center frequencies of the measured lines varied from 8662.0 MHz to 48612.70 MHz.

All experimentally measured line width's $\Delta\nu$, were corrected for broadening due to Modulation and Doppler effects. No corrections had to be made for line broadening due to saturation effects, collisions with the walls of the cell, etc. as their contribution to the line width is negligible.

Line width parameters $\Delta\nu_p$, for the several observed transitions were determined by graphing half-widths versus pressure for each spectral line, and performing a linear least-square fit on the data points. Repeatability measurements indicated the accuracy of the line width parameters to be better than ± 7 per cent. Broadening of each spectral line was measured for self broadening and foreign-gas

broadening by atomic helium and diatomic hydrogen. Effective collision diameters were calculated for each broadening interaction, based on the observed rates of broadening.

Measurements on the formic acid system indicate that, for self broadening interactions, there is a dependence of the collision diameters on the quantum number J. The collision diameters (for HCOOH-HCOOH interactions) were found to be approximately constant (12.3 Å) for $J \leq 12$, then to decrease in the range $3 \leq J \leq 32$. Collision diameters for He and H_2 were found to be approximately constant over the range $3 \leq J \leq 32$.

For the formaldehyde system, the self broadening collision diameters (at low pressures) were found to vary in magnitude from 11.70 - 15.90 Å over the range $7 \leq J \leq 25$. Diameters due to foreign-gas (He and H_2) broadening also displayed fluctuations for the different lines over the range $7 \leq J \leq 25$.

The experimentally determined collision diameters for self broadening interactions involving HCOOH and CH_2O molecules were found to be 2 - 27 per cent less than those calculated by the Murphy-Boggs theory of collision broadening. Much better agreement between a simplified broadening scheme for symmetric top molecules and the observed foreign-gas collision diameters is obtained by using Birnbaum's theory.

For a number of CH_2O lines an anomalous behavior was observed in some of the graphs of half-widths versus pressure. Namely, the slope of the graphs occasionally changed abruptly at a particular pressure. This effect was found to be pressure and temperature dependent and a possible explanation based on collisional pumping of rotational levels is discussed.

TABLE OF CONTENTS

LIST OF TABLES

LIST OF ILLUSTRATIONS

CHAPTER I

INTRODUCTION

Although one can trace the beginning of microwave spectroscopy to the historic experiments of Cleeton and Williams[1] in 1934 on the inversion spectrum of ammonia, no further papers appeared in the literature until 1946. The concentrated research on microwave radar during World War II provided the necessary instrumentation and the stimulus for a rapid development of this field of spectroscopy during the past three decades. Absorption spectroscopy in the microwave region has revealed not only new information on intermolecular interactions but has provided researchers with an extremely precise method of obtaining important molecular and nuclear parameters. Some of the parameters which can be obtained from microwave analysis are bond angles, interatomic distances, molecular dipole and molecular quadrupole moments, atomic masses, nuclear spins, and nuclear quadrupole moments.

The microwave region comprises that part of the electromagnetic spectrum which lies between the far infrared and the conventional radio frequency region. Though its boundaries are not precisely fixed, the region may be regarded as extending from about 1 mm to 30 cm in wave length

(300,000 MHz to 100 MHz in frequency). One may also define the microwave region on the basis of the type of spectral studies to which it is best suited. Bearing in mind a number of outstanding exceptions, I may say that in the microwave region transitions between rotational energy levels are directly observed with nuclear effects appearing as first order perturbations.[2] As examples of the exceptions mentioned above, there are differences between certain electronic energy levels which fall within the microwave region. The most notable example of this is the Lamb-Retherford shift[3] in the spectrum of hydrogen. There are also a few outstanding examples of certain light molecules like HCl and NH_3 for which pure rotational lines have been measured in the far infrared region. Nevertheless, by far the greater proportion of pure rotational lines are measurable in the microwave region only.

Two restrictions are commonly placed on molecules which exhibit pure rotational absorption spectra: (1) they must possess a permanent dipole moment (with certain exceptions of induced dipole moments in non-polar liquids), and (2) they should have sufficient vapor pressure to give an observable microwave spectrum. The first restriction is imposed because the intensity of a rotational spectral line is directly proportional to the square of the dipole moment matrix element[4] connecting the two rotational levels in question. The second restriction is also essential since

extremely high resolution is achieved only with gaseous samples.[5] Despite these two restrictions there are large classes of compounds to which microwave analysis is possible.

A basic apparatus for observing microwave absorption spectra is shown in Figure 1. The source of radiation (a klystron) is varied in frequency by a saw-tooth voltage pulse in such a way that the frequency output produces time varying signals from the molecular transitions being induced. As the frequency of the source is swept through a frequency corresponding to an allowed transition within the molecule present in the absorption cell, a part of the radiation is absorbed by the molecule. This absorption appears as a power "dip" at the detector (generally a crystal diode). Application of the time varying saw-tooth to the radiation will produce a display on the read-out device, here an oscilloscope. The apparatus shown in Figure 1 is very basic and gives only the minimum requirements for doing microwave spectroscopy. A more detailed description of the microwave spectrometer used in this study is given in chapter V.

Since the rotational motion of a molecule is quantized, transitions between rotational energy levels are characterized by well defined resonances or spectral line "shapes." Figure 2 shows a typical resonance pattern for a rotational energy transition in the microwave region. Microwave spectral lines at low pressures ($P < 1$ atm.) have a Lorenztian shape.[6]

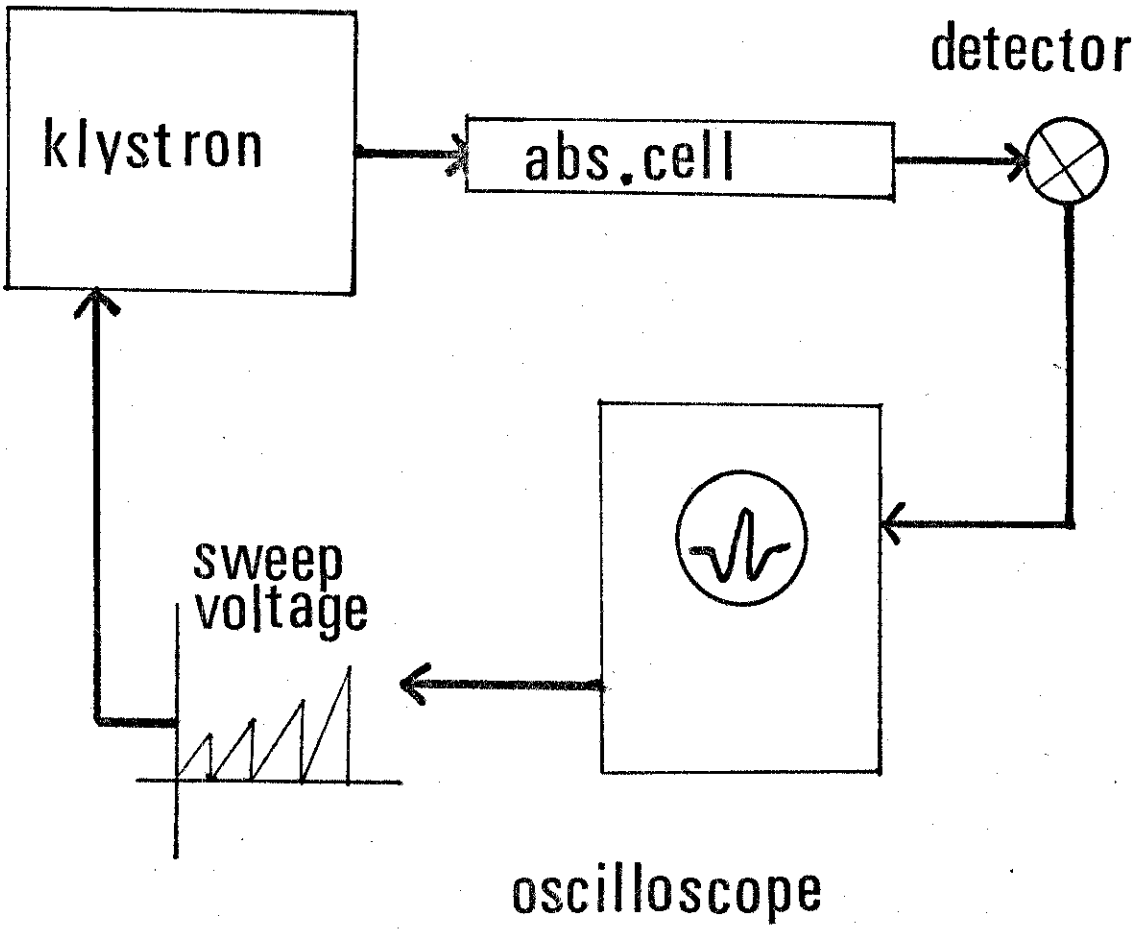

Fig. 1. Basic apparatus for observing microwave spectra.

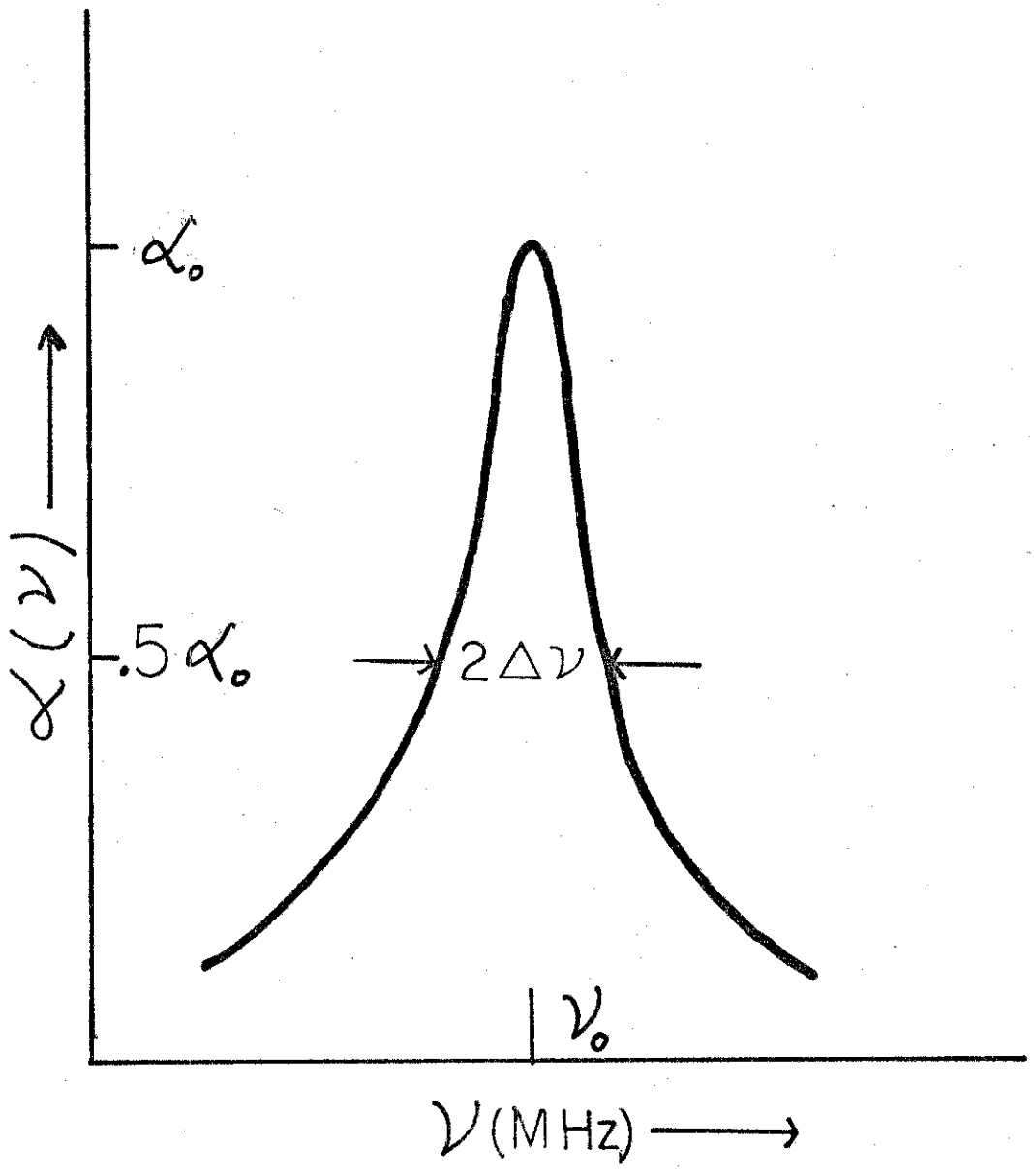

Fig. 2. Absorption profile of a Lorentzian line shape.

The frequency at maximum absorption, α_0, is known as the line frequency of the transition and is normally labelled ν_0. The total frequency width of the line at half maximum absorption is denoted by $2\Delta\nu$, where $\Delta\nu$ is referred to as the half width of the spectral line.

From a systematic and precise determination of half widths of spectral lines it is possible to infer interaction parameters and interaction processes which take place between molecules being observed. Two groups of interactions are generally studied. These can be broadly classified under the headings "self-broadening" and "foreign-gas broadening."

When investigations of self broadening are being made all the molecules within the absorption cell are of one kind. On the other hand, in the foreign gas broadening scheme interactions between different types of molecules are studied. In these investigations the quantity of physical importance is the "line width parameter" denoted by $\Delta\nu_p$. This quantity is the slope of the curve obtained by plotting $\Delta\nu$ against pressure. From a knowledge of $\Delta\nu_p$ along with other molecular parameters it is possible to deduce an effective collision diameter for interactions between the type molecules being studied.

The molecules under investigation in this study are formaldehyde (also known as methanal or oxomethane) and formic acid (also known as methanoic acid). Both CH_2O and HCOOH are planar, near-prolate asymmetric top molecules

(i.e., no two principal moments of inertia are equal, but the two largest moments are approximately equal). The structures of CH_2O and HCOOH in their electronic ground states are shown in Figures 3 and 4 respectively.

Formaldehyde is a gas at temperatures above -19°C, although it has a tendency to polymerize[7] at temperatures near 100°C. It has a large permanent dipole moment[8] of 2.34 Debyes (1 D = 10^{-18} esu) parallel to the a-axis (i.e., the axis of smallest inertial moment), and has a rotational spectrum in the microwave region.

On the other hand, formic acid is a liquid at room temperatures with an appreciable vapor pressure (~10.96 Torr ar 300°K). Unlike formaldehyde, formic acid has components of the permanent dipole moment both parallel and perpendicular to the axis of the smallest inertial moment (the a-axis). The direction of the dipole moment is shown in Figure 4. The magnitude[9] of the total dipole moment is 1.415 Debyes. The two components (μ_a and μ_b) have magnitudes 1.39 Debyes and 0.26 Debyes respectively. Due to the small magnitude of μ_b, all transitions dependent on this component of the dipole moment are extremely weak and only a few have been observed.[10] Only μ_a-type transitions have been studied in this investigation. Like formaldehyde, formic acid has a rotational spectrum in the microwave region. Consequently, it can be studied by microwave techniques.

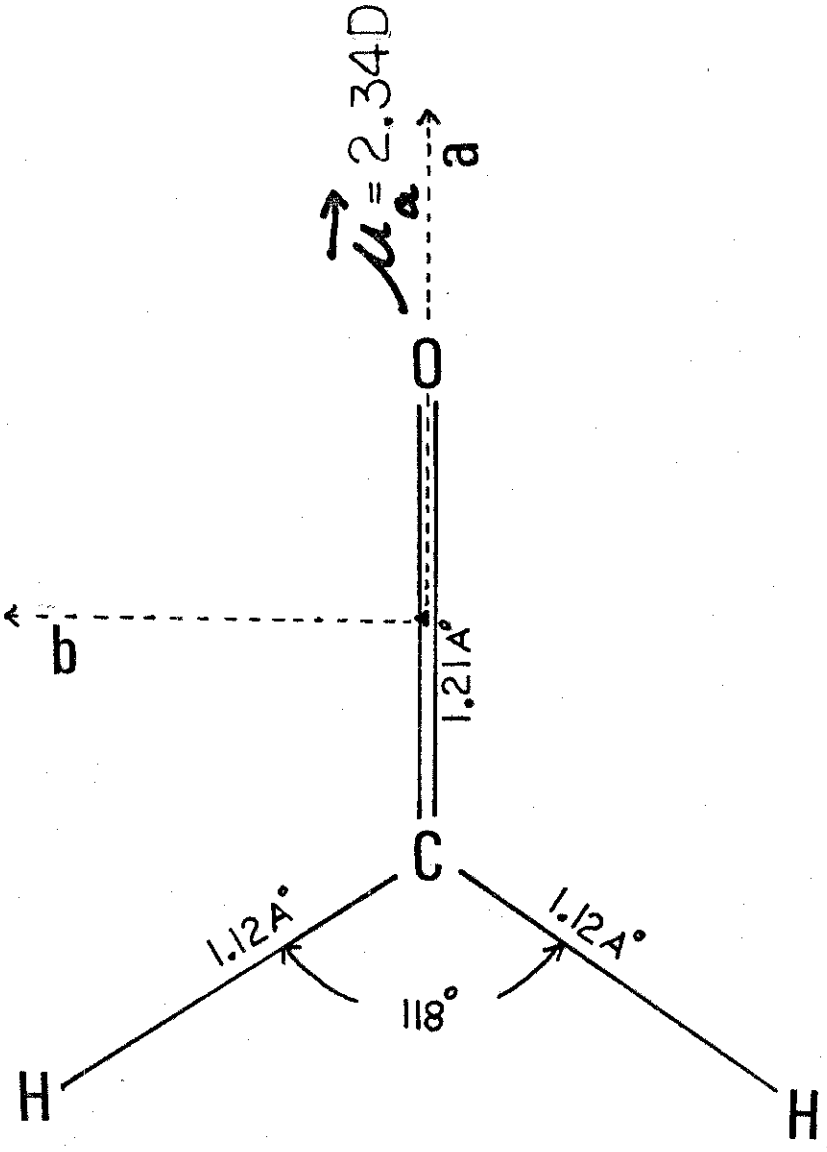

Fig. 3. Electronic ground state structure of monomeric formaldehyde.

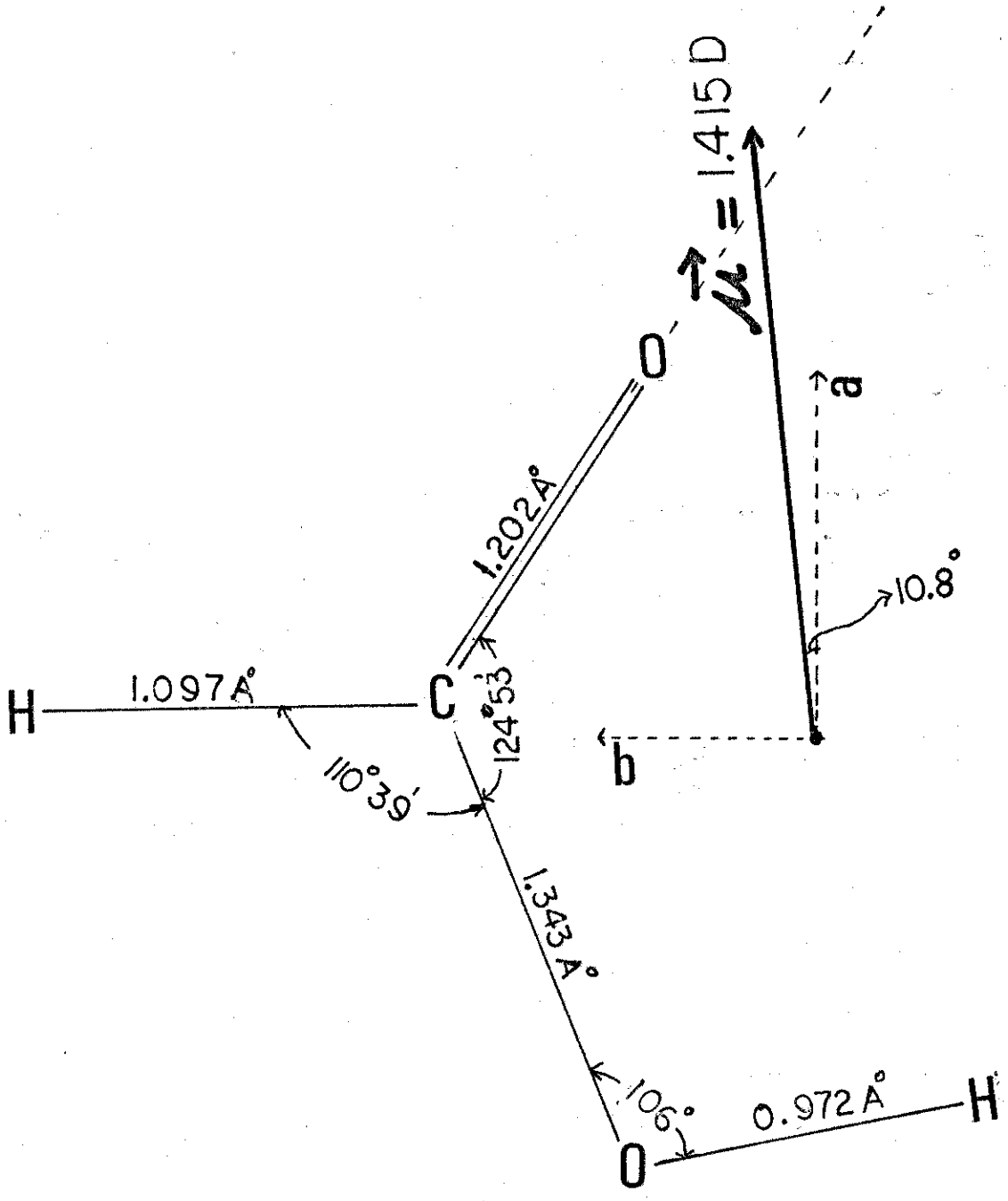

Fig. 4. Electronic ground state structure of formic acid.

The purpose of this investigation is to study the effects of pressure broadening (both self and foreign gas) on a number of Q branch ($\Delta J=0$) transitions in the rotational spectrum of formaldehyde and formic acid. An incentive to carry out this investigation has been provided by the recent discovery[11] of complex molecules (including CH_2O and HCOOH) in interstellar space, which are observed to have anomalous distributions in their rotational energy states. There is reason to believe that such an anomalous distribution may be caused by molecular collisions.[12] Microwave collision diameters obtained from pressure broadening experiments should prove useful in establishing this collision mechanism for anomalous distribution. Also, these collision diameters (or collision cross sections) are useful to astrophysicists studying formation rates of interstellar CH_2O and HCOOH. Finally, pressure broadening studies on these molecules should shed light on the nature of the intermolecular forces involved when self collisions (i.e., CH_2O-CH_2O and HCOOH-HCOOH) and foreign gas collisions of CH_2O and HCOOH with H_2 and He take place.

This dissertation is divided into five chapters. Chapter II contains a brief survey of the previous microwave studies on CH_2O and HCOOH. The shape of microwave spectral lines and the various broadening mechanisms (except pressure broadening) are discussed in Chapter III. In Chapter IV, the various

theories of pressure broadening are reviewed. A description of the pertinent experimental apparatus used in this investigation can be found in Chapter V. And finally, Chapter VI contains the presentation and the analysis of the experimental data obtained in this investigation.

CHAPTER II

BACKGROUND

CH_2O

Bragg and Sharbough[13] were the first investigators to study formaldehyde in the microwave region. They observed and assigned a few lines to the K-doubling transitions in the rotational spectrum of CH_2O. (K-doubling refers to the splitting of rotational energy levels in asymmetric top molecules that occurs when the K-degeneracy is removed by "turning on" the asymmetry; K is the quantum number for the component of the angular momentum J along the molecular axis in symmetric rotors.) The problem of centrifugal distortion in CH_2O was studied in detail by Lawrence and Strandberg.[14] In the past ten years a number of investigators have measured the frequency of many microwave transitions (down to the millimeter wavelengths) so that the rotational spectrum of CH_2O is well known.[15,16] In addition, magnetic hyperfine structures that appear in the K-doubling transitions as a result of the proton spin interactions with the magnetic field due to molecular rotation have been experimentally measured[17] and also examined theoretically.[18]

In recent years a number of complex molecules (including CH_2O) have been discovered in interstellar space.[11] Absorption

of the isotropic radiation of 4830.0 MHz by the ($1_{11} \rightarrow 1_{01}$) rotational transition of formaldehyde in cool dust clouds in our Galaxy have been reported by Palmer et al.[19] They point out that this absorption implies an effective temperature for these two levels below the temperature of both isotropic radiation and the expected kinetic temperature. Such an excess population in the lower state 1_{11} requires a non-thermal cooling mechanism, just as maser action in OH and H_2O requires a non-thermal excitation temperature. Townes and Cheung[12] have proposed molecular collisions as a possible mechanism for the above mentioned maser effect.

Pressure broadening studies for a number of CH_2O transitions have been carried out by Rogers and Roberts.[20] They observed transitions of the type $\Delta J = 0$ (i.e. Q-branch transitions) with $1 \leq J \leq 5$. Pressure ranges from 0.001-0.1 Torr were explored in obtaining line width parameters $\Delta\nu_\rho$ for each transition. The collision diameters obtained from the experimentally determined $\Delta\nu_\rho$ were found to be constant (14.0 A°) for CH_2O - CH_2O interactions, 2.5 - 5.8 A° for CH_2O - H_2 interactions and 2.7 - 3.5 A° for CH_2O - He interactions.

HCOOH

Formic acid was first studied in the microwave region by Rogers and Williams[21] in order to obtain the structure of the molecule. Although they were able to establish the

planarity of the HCOOH molecule, their values for the interatomic distances and bond angles were found to be in wide disagreement with the values obtained from electron and x-ray diffraction[21] data. Lerner et al.[22] analyzed the microwave spectrum of five isotopic species of formic acid to arrive at the present known structure of the molecule (with excellent agreement with electron and x-ray diffraction data). Bellet et al.[23] have examined the problem of centrifugal distortion in the HCOOH molecule and also measured the frequencies of a large number of Q-branch ($\Delta J = 0$) and R-branch ($\Delta J = +1$) transitions in the microwave region. The dipole moment of formic acid has been precisely determined by Kim et al.[9] using the Stark effect. Their results confirm the fact that the dipole moment has components both parallel and perpendicular to the a-axis (axis of smallest inertial moment).

Like formaldehyde, formic acid has also been detected in interstellar space. Zuckerman et al.[24] have observed an emission line in the direction of Sgr B2, and identified it as the ($1_{10} \longrightarrow 1_{11}$) transition of interstellar HCOOH at a frequency of 1638.8 MHz. The authors point out the fact that since the formic acid line is observed in emission, either the excitation temperature describing the relative population in the 1_{11} and 1_{10} levels is greater than 150°K (the continuum background temperature) or negative. In

either case, it appears that the relative populations in 1_{11} and 1_{10} are determined by processes other than ordinary kinetic collisions, since kinetic temperatures in dense interstellar clouds are generally believed to be less than 150°K.

CHAPTER III

LINE SHAPES AND LINE BROADENING

A perfectly isolated, undisturbed, and stationary molecular system would be characterized by definite and fixed energy levels, but various unavoidable disturbances exist which tend to vary the energy levels, giving a width to spectral lines and varying their mean or central frequencies. The various sources of spectral line broadening may be listed as:

1. Natural line width
2. Doppler effects
3. Pressure broadening
4. Collisions with the walls of the absorption cell
5. Saturation broadening
6. Modulation broadening
7. Overlapping of spectral lines

Since the purpose of this study is the investigation of pressure broadening effects on rotational spectral lines, all other sources of line broadening have to be first accounted for before one can obtain pressure broadened line widths. A number of the sources of broadening listed above can either be ignored (since they are small in magnitude) or experimentally minimized; corrections based on theoretical

arguments have to be made on the remaining sources of line broadening. All such corrections depend upon the shape of the spectral line. In the following section, a brief account of the microwave spectral line shapes is given. Following this, a detailed account of the sources of line broadening (except pressure broadening) with emphasis on their origin is discussed. In addition, the procedure used to arrive at numerical corrections for broadening due to Doppler effects, modulation effects, and overlapping spectral lines is also given.

Line Shapes

Low pressure microwave spectral lines are observed to be symmetrical about their center frequency (Figure 1). On theoretical grounds the shape of these lines has been generally assumed to be Lorentzian. The Lorentzian shape has been confirmed experimentally by the work of Netterfield et al.[25] on a number of rotational lines of ammonia. It is further observed that in most molecules (including CH_2O and HCOOH) the Lorentzian shape is "approximately" retained even in the presence of the various broadening mechanisms listed above. Doppler effects and overlapping spectral lines are the principal sources which can cause appreciable distortion of the Lorentzian line shape.

The Lorentzian line shape was first predicted by Lorentz for pressure broadened lines.[16] He treated the molecules as

radiators that undergo random phase changes on collisions. Lorentz's theory was found to be good only in the cases where the line widths were smaller than the resonance frequency. Van Vleck and Weiskoff[27] modified the Lorentz theory by assuming that the radiation phases are not completely random but are determined by equilibrium Boltzmann distribution. The Van Vleck-Weiskoff theory predicts the right shape for all ratios of the line width to the resonant frequency and also over a wider pressure range.[28] Although, Van Vleck and Weiskoff's theory is based on classical reasonings a quantum mechanical treatment gives identical results.[29] The absorption coefficient based on the Van Vleck-Weiskoff theory is given by [30]

$$\alpha(\nu) = \frac{8\pi^2 fN}{3ckT} |\mu_{ij}|^2 \nu^2 \left[\frac{\Delta\nu}{(\nu-\nu_0)^2+(\Delta\nu)^2} + \frac{\Delta\nu}{(\nu+\nu_0)^2+(\Delta\nu)^2} \right], \quad (1)$$

where N is the total number of molecules per unit volume, f the fraction of molecules in the lower energy state, μ_{ij} the dipole moment matrix element connecting the two states in question, ν_0 the resonant frequency, and $\Delta\nu$ the half width at half maximum of the spectral line. The constants c and k have the usual meaning with T, the temperature, usually fixed at a constant value for the experiment.

At low pressures (where $\Delta\nu << \nu_0$), the first term in equation (1) is the predominant one and the expression for $\alpha(\nu)$ reduces to

$$\alpha(\nu) = \frac{8\pi^2 Nf}{3ckT} |\mu_{ij}|^2 \nu^2 \Delta\nu \{(\nu-\nu_0)^2 + (\Delta\nu)^2\}^{-1}. \quad (2)$$

Furthermore, the presence of the factor ν^2 in equation (2) does not affect the line shape as long as $\Delta\nu << \nu_0$.[30] Hence, for narrow microwave spectral lines the frequency dependence for the line shape may also be written as

$$F(\nu) \propto \{(\nu-\nu_0)^2 + (\Delta\nu)^2\}^{-1}, \quad (3)$$

with $\Delta\nu$ being constant at a given temperature.

Experimentally, one generally observes derivatives of the absorption profile, $\alpha(\nu)$. Figure 5 shows the Lorentzian profile and the first and second derivatives of the profile. The chief advantage of using these derivatives is the ease with which the half-power points can be established. It is a simple matter to show that peaks of the first derivative are related to the half-width $\Delta\nu$ by $2\delta\nu = \frac{2\Delta\nu}{3}$ where, following convention, the distance between peaks of the derivatives is denoted by $\delta\nu$. The peaks of the second derivative coincide with the half-power points of $\alpha(\nu)$: $2\delta\nu_2 = 2\Delta\nu$. It should be noted that the relation between $\Delta\nu$ and $\delta\nu$ applies only when the line is Lorentzian and the amplitude of the modulating signal applied to produce the derivatives is small.

Natural Line Width

The natural line width may be interpreted as due to radiation damping, or quantum mechanically as the disturbance

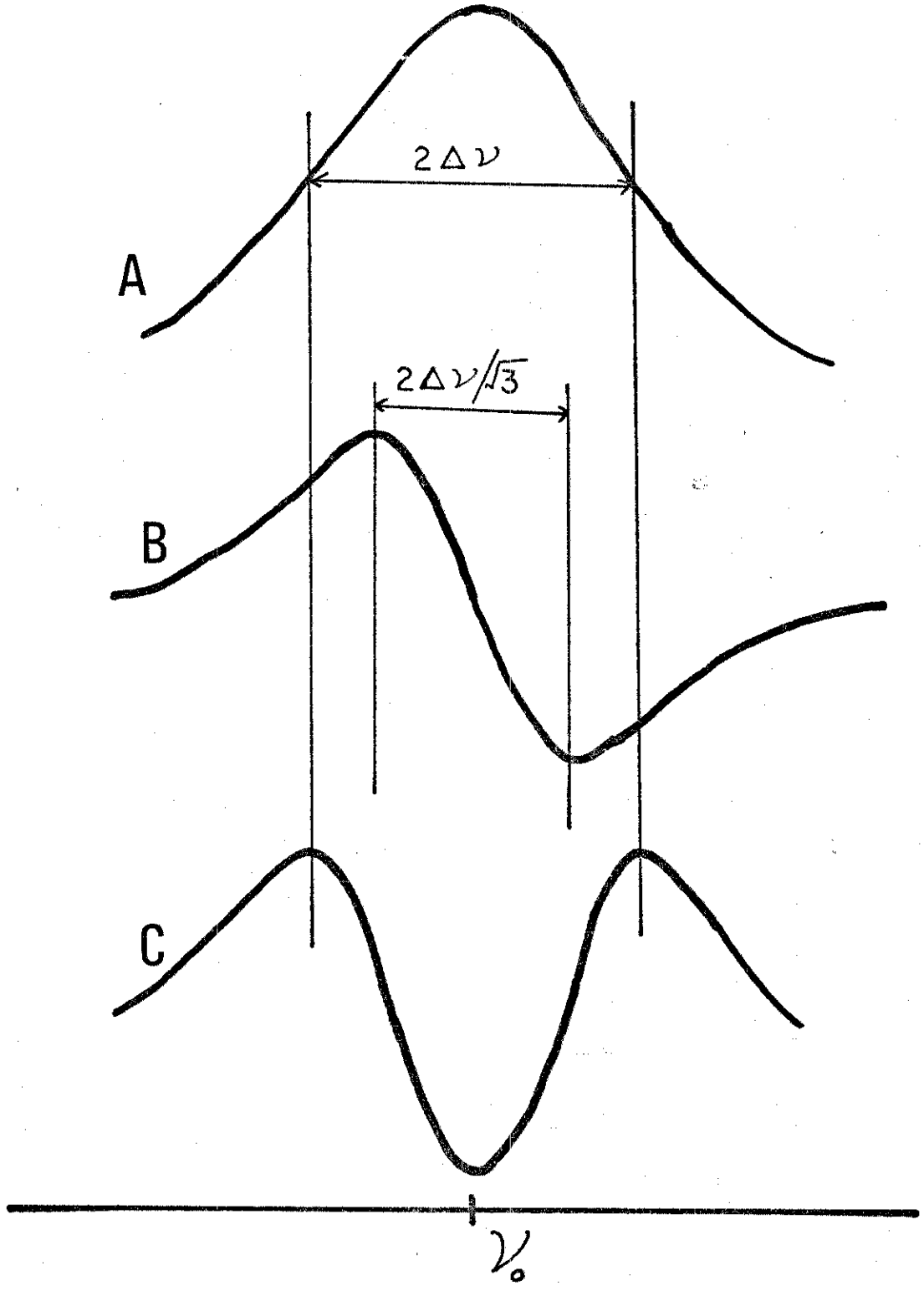

Fig. 5. Profiles of a Lorentzian and its first two derivatives. (A) Lorentzian line shape; (B) First Derivative; (C) Second derivative profile.

of the molecule by zero-point vibrations of electromagnetic fields which are always present in free space. For a transition of frequency ν from an excited state to the ground state of the system, zero-point electromagnetic fields give an absorption line a half width[31] at half maximum intensity of

$$\Delta\nu = \frac{32\pi^3\nu^3}{3hc^3} |\mu|^2 , \qquad (4)$$

where μ is the quantum-mechanical matrix element of the dipole moment. For microwave frequencies and ordinary temperatures thermal radiation consists of stronger electromagnetic fields than the usual zero-point fields, since each mode of vibration of the field has a mean energy kT rather than $h\nu/2$. This increases the value of $\Delta\nu$ above by a factor of $2kT/h\nu$,[31] or approximately 400 at room temperature.

An estimate for the value of the natural line width for CH_2O may be obtained by substituting appropriate values for μ and ν in Equation (4) above. The dipole moment of CH_2O is 2.34 Debyes, and, using a typical frequency of 30 GHz for ν, the value for $\Delta\nu$ is found to be 1.8×10^{-4} KHz. Similarly, one can also estimate the natural line width for HCOOH (for the same frequency, ν) by substituting μ=1.39 Debyes in Equation (4). This gives a value of 8.5×10^{-5} KHz for $\Delta\nu$ at room temperature. These widths are quite small in comparison to those due to other broadening mechanisms

(observed line width's for CH_2O and HCOOH are generally in the range 50 → 200 KHz). Therefore, no corrections have to be made for broadening due to the presence of stray electromagnetic fields.

Doppler Effect

The Doppler effect occurs when a molecule is moving parallel to the direction of propagation of the radiation being absorbed. There is an apparent shift in the radiation frequency, as seen by the moving molecule, given by[32]

$$\delta\nu' = \pm\nu(v/v_p) \quad , \tag{5}$$

where ν is the frequency of the radiation, v the velocity of the molecule, and v_p the phase velocity of the incident radiation.

Doppler broadening does not become dominant until the pressure of the gas in the absorption cell is reduced to a small value. At these low pressures the molecules are able to travel more freely; hence, they describe longer paths (before they collide with one another) as compared to the paths that they travel at higher pressures. The Doppler contribution to the line width approaches a constant value at higher pressures. Therefore, for low pressure studies on spectral lines in the microwave region (as in this investigation) the Doppler effect becomes one of the dominant width factors. This contribution to the line width has to be

considered if accurate pressure broadened line widths are required. Parsons and Roberts[33] have worked out a correction procedure to compensate for the line width error due to Doppler broadening. An analysis of their correction procedure is given below.

If radiation of frequency ν in the lab frame of reference is incident in the x-direction on molecules whose x-component of velocity is v_x, the frequency relative to these molecules is given by [from Equation (5)]

$$\nu' = \nu\left(1 \pm \frac{v_x}{c}\right) . \tag{6}$$

The number of molecules per unit volume will be given by the Maxwellian distribution[33]

$$\delta N_{v_x} = N\left[\frac{m}{2\pi kT}\right]^{\frac{1}{2}} e^{-\frac{mv_x^2}{2kT}} \delta v_x . \tag{7}$$

The contribution that they make to the absorption coefficient $\alpha(\nu)$ is given by the Van Vleck-Weiskoff equation at low pressures [i.e. Equation (2)]

$$\delta\alpha(\nu) = \frac{8\pi^2 f |\mu_{ij}|^2}{3ckT} \nu'^2 [(\nu'-\nu)^2 + (\Delta\nu)^2]^{-1} \delta N_{v_x} \Delta\nu , \tag{8}$$

with the line shape profile obtained by integrating Equation (8) to obtain the total contribution of all the elements to the line shape.

For microwave transitions at low pressures, the approximate[33] line shape

$$\alpha(\nu) = A(T)N\Delta\nu \int_0^\infty \frac{\exp\{-\beta(\nu-\nu')^2\}}{(\nu'-\nu_0)^2+(\Delta\nu)^2} d\nu' \qquad (9)$$

is obtained by combining equations (6), (7), and (8). A(T) is a constant characteristic of the gas at a given temperature and $\beta=mc^2/2kT\nu_0^2$.

Values for $\alpha(\nu)$ have been calculated from Equation (9) and plotted in Figure 6, as a function of ν for a proper molecular transition with ν_0=25.0 GHz. This line shape profile was calculated at a temperature of 27°C. To make a comparison between the true line shape and the distorted line shape, the corresponding Lorentzian shape is also plotted, after proper normalization, so that the peaks of the two curves coincide. Examination of the two curves clearly reveals that line width measurements at low pressures will yield larger line widths than should be observed.

For Figure 5 the peaks of the first derivative profile correspond to the points of steepest slope of the function $\alpha(\nu)$. Thus the second derivative of $\alpha(\nu)$ can be used to get the critical points of the first derivative. Equating the second derivative of $\alpha(\nu)$ with respect to ν of Equation (9) to zero gives

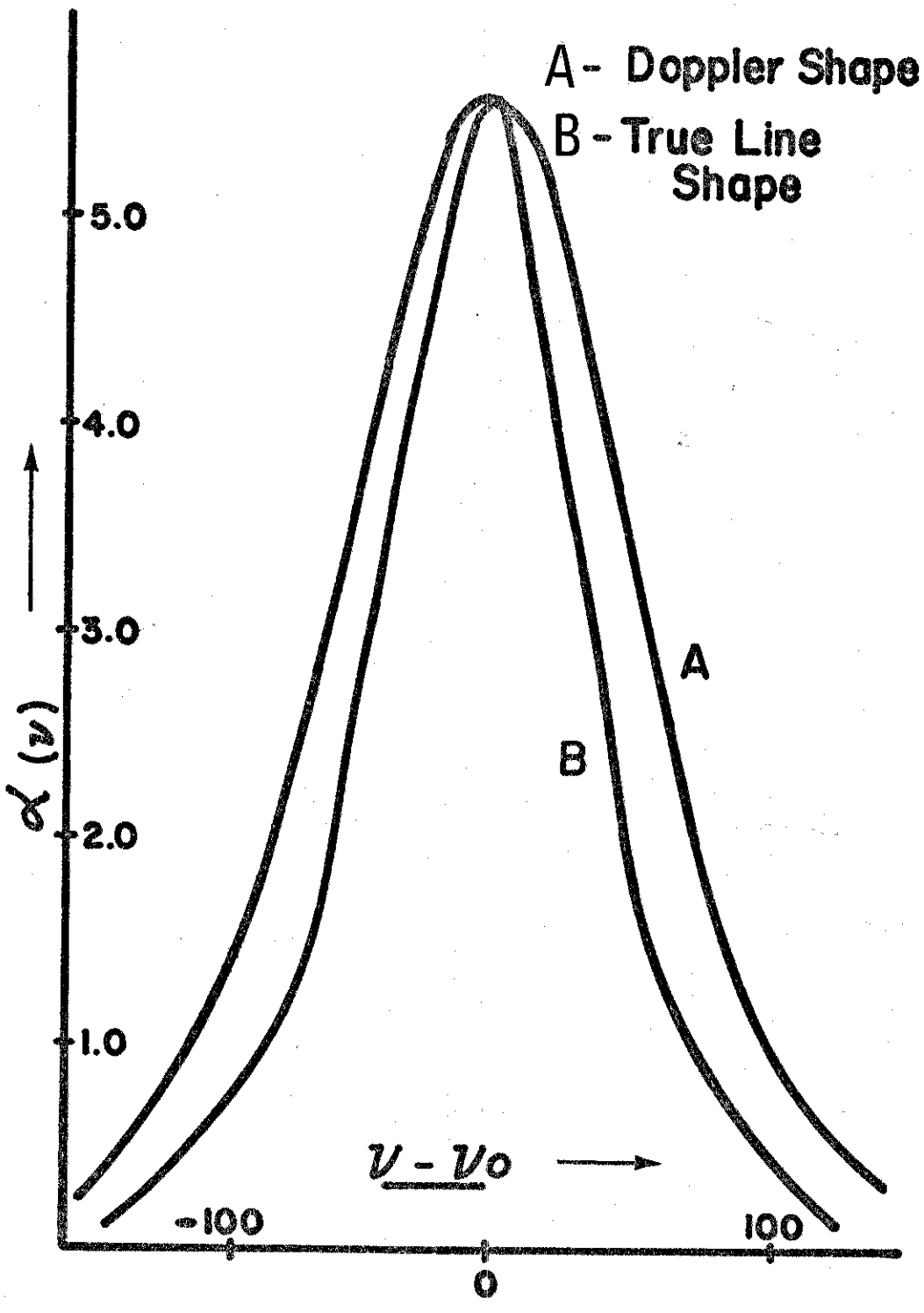

Fig. 6. Line profile for Doppler and non-Doppler broadened spectral line of Lorentzian shape.

$$\int_0^\infty \frac{(1-2\beta x^2)\exp(-\beta x^2)}{(x+\nu-\nu_0)^2+(\Delta\nu)^2}dx \equiv 0 \ , \tag{10}$$

where the substitution $x=\nu'-\nu$ has been made. Equation (10) allows one to determine where the peaks of the first derivative of $\alpha(\nu)$ are located for a line which is both pressure and Doppler broadened.

Denoting the points of steepest slope of $\alpha(\nu)$ by $\nu=\nu_0\pm\delta\nu$ Equation (10) becomes

$$\int_0^\infty \frac{(1-2\beta x^2)\exp(-\beta x^2)}{(x\pm\delta\nu)^2+(\Delta\nu)^2}\, dx \equiv 0 \ . \tag{11}$$

Therefore, given the absolute temperature, the central frequency ν_0, and the mass m of the molecule under study, Equation (11) can be solved for the values of $\delta\nu$ that give a zero integral for any value of $\Delta\nu$. Solutions of Equation (11), using $\Delta\nu$ as a parameter, are best obtained using the Gauss-Hermite quadrature method of numerical integration, which is defined by[34]

$$\int_{-\infty}^{\infty} e^{-x^2} f(x)dx = \sum_i w_i f(x_i) \ , \tag{12}$$

where the roots x_i and weight factors w_i are obtained from tables.[35] A computer program has been written for an IBM 360/50 computer to solve Equation (11) for the value of $\delta\nu$ that correspond to any value of $\Delta\nu$.

The correction that must be applied to the second derivative of the line shape (as used in this investigation) to take into account the Doppler broadening is given by

$$C = \delta\nu - \Delta\nu \ . \qquad (13)$$

Correction curves obtained by plotting C against $\delta\nu$ for a number of transition frequencies of formaldehyde and formic acid are shown in Figures 7 and 8 respectively. From the shape of these corrections curves it is evident that the correction $\delta\nu-\Delta\nu$ is always greater for smaller $\delta\nu$ (i.e. lower pressures). Therefore, the Doppler correction always increases the slope of the plot of $\Delta\nu$ versus P over the uncorrected $\Delta\nu_p$. This can be seen in Figure 9 where both the uncorrected line widths as well as the Doppler corrected line widths have been plotted against pressure for the $9_{2,8} \longrightarrow 9_{2,7}$ transition of CH_2O. Doppler correction for the line width data results in an increase in slope from 16.72 MHz/Torr to 19.0 MHz/Torr for this particular transition. Similar increases in slope are observed for all the lines studied in this investigation.

Although the Doppler correction discussed above is based purely on theoretical arguments, experimental evidence based on our measurements confirm the validity of Equation (11). We have found the Doppler corrected line widths fall more closely along a straight line than do uncorrected line

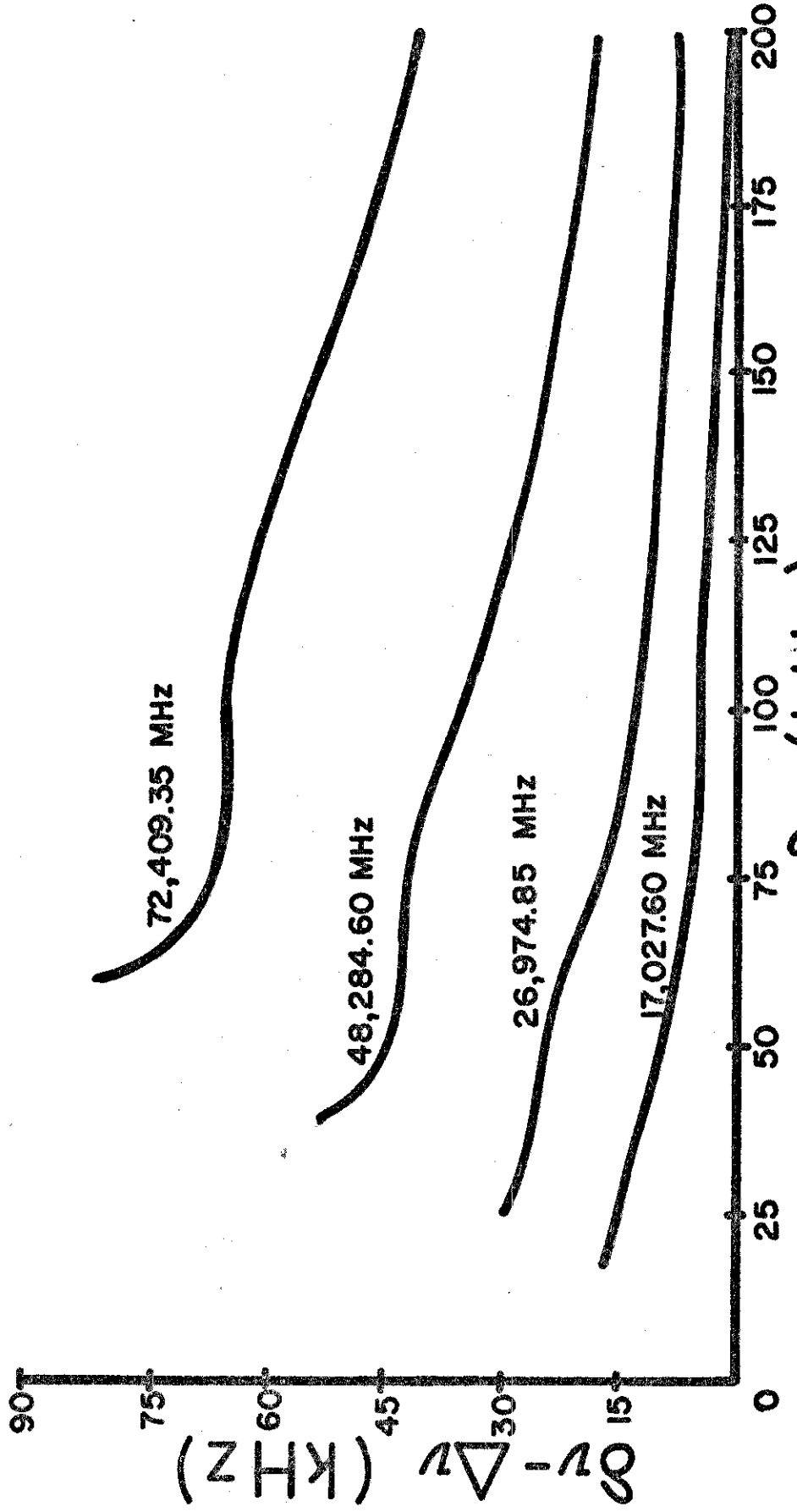

Fig. 7. Doppler correction curves for formaldehyde spectral lines.

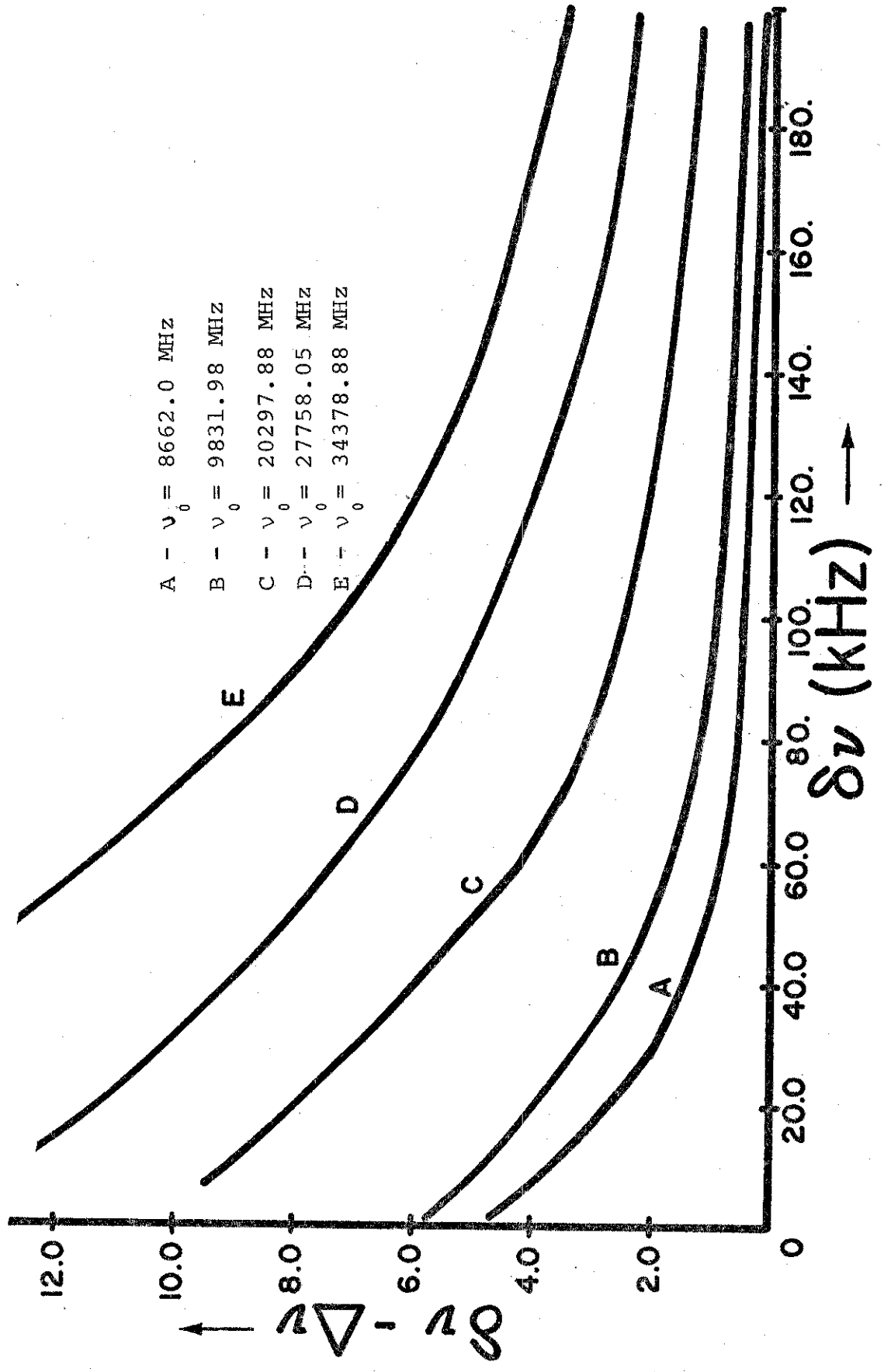

Fig. 8. Doppler correction curves for formic acid spectral lines.

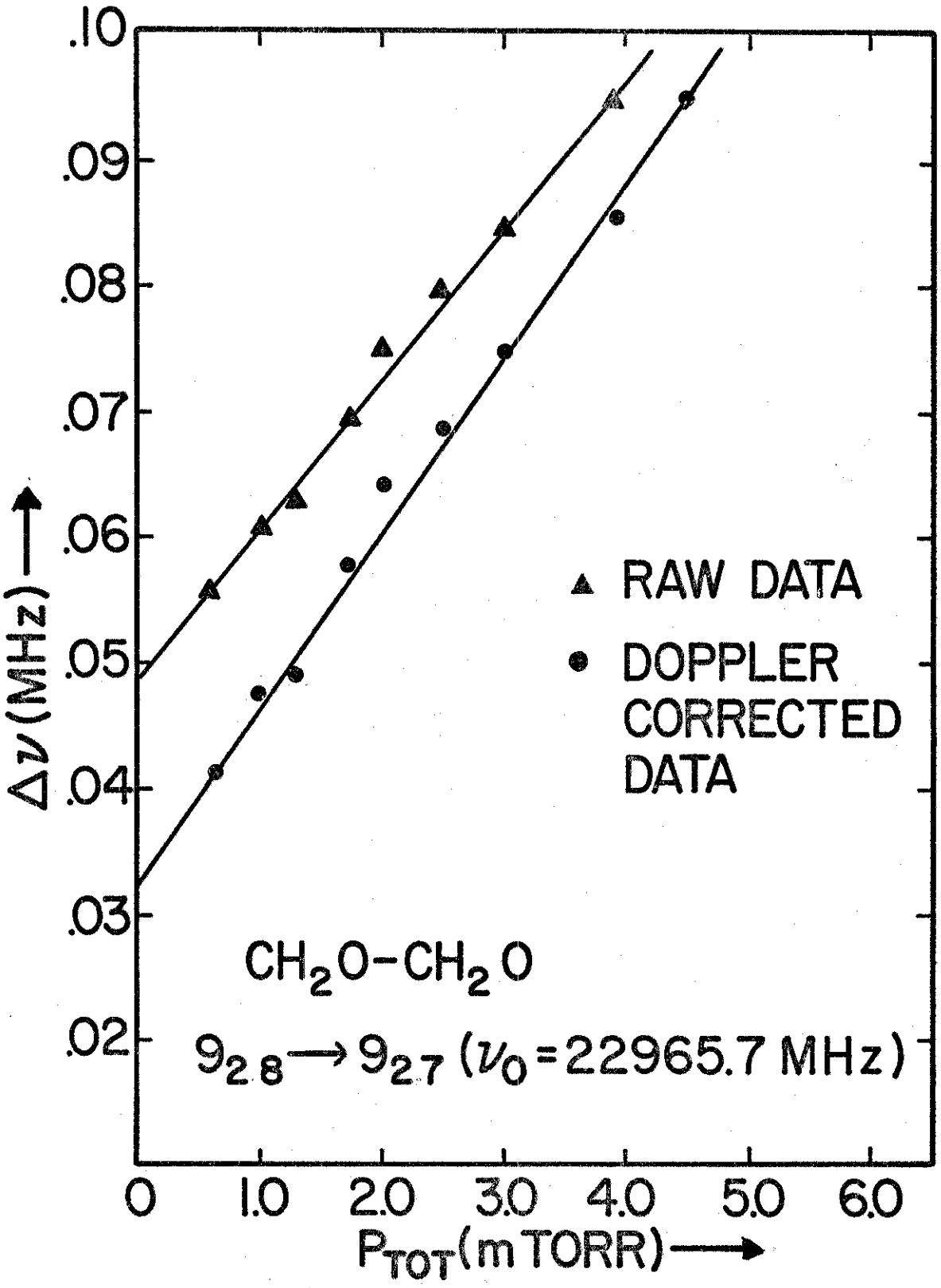

Fig. 9. Line width parameter curves for the $9_{2,8} \longrightarrow 9_{2,7}$ transition of CH_2O.

widths when plotted against pressure. In addition, it was found that the rms deviation of the experimental points from the best-fit straight line was reduced if the points were first corrected for Doppler broadening.

Wall Broadening

Danos and Geschwind[36] have analyzed the problem of broadening of microwave spectral lines due to collisions of the molecules with the walls of the absorption cell. Their expression for the wall broadened half width in a cell having circular cross section is given by

$$\Delta\nu = \frac{1.25}{4a}\left(\frac{2kT}{m}\right)^{\frac{1}{2}} \quad , \tag{14}$$

where a is the radius of the cell and m the mass of the molecule being studied. The cell used had a radius of 2.5 cm and the mass of the CH_2O molecule is 5.0×10^{-25} gm. Substituting these values in Equation (14) gives $\Delta\nu$=2.4 KHz at 27°C.

For HCOOH, a rectangular cell was used. For such a cell, the wall broadened line width is given by[37]

$$\Delta\nu = \frac{1}{3\pi}\left(\frac{a+b}{ab}\right)\left(\frac{2kT}{m}\right)^{\frac{1}{2}} \quad , \tag{15}$$

with a=1.8 cm and b=2.5 cm. Substituting the mass of HCOOH in Equation (15) gives $\Delta\nu$=1.90 KHz at 27°C. Since wall

broadened line widths are small (compared to other sources of broadening), no corrections had to be made for this source of broadening.

Saturation Broadening

Effects of saturating the molecules with resonant radiation were first discovered in the microwave region by Townes[38] and Bleaney and Penrose.[39] The principal results of saturation are a decrease in the absorption coefficient and a broadening of the absorption line. These effects, which result from a disturbance of the thermal equilibrium, have been confirmed a number of times[40,41] and theoretically explained by Karplus and Schwinger.[42]

Saturation effects become evident when the incident power is sufficient to lift molecules from the lower to the higher state at a rate comparable with their return to the former state. Since collisions with other molecules are the principal mode of relaxation of the molecules, the effects become significant only at relatively low pressures.

The maximum power that can be absorbed by the molecules is given by the expression[37]

$$P_{max} = 1/2[(N_1-N_2)/\tau]h\nu \ , \qquad (16)$$

where N_1 and N_2 are the populations of the two states considered, τ is the average relaxation time, and $h\nu$ is the energy difference between the states. In the absence of

saturation the population densities of the two states are related by the equilibrium Boltzman distribution

$$N_2 = N_1 \exp(-h\nu/kT) \quad , \tag{17}$$

with the difference in population densities given by

$$N_1 - N_2 = N_1[1-\exp(-h\nu/kT)] \quad . \tag{18}$$

Combining Equations (16) and (18) gives

$$P_{max} = N_1 \frac{[1-\exp(-h\nu/kT)]}{2\tau} h\nu \quad . \tag{19}$$

Since $h\nu << kT$ for microwave radiation, the exponent in Equation (19) may be expanded, i.e.,

$$P_{max} \approx \frac{N_1 (h\nu)^2}{2\tau kT} \quad . \tag{20}$$

Using the above definition for P_{max}, Carter and Smith have shown that the absorption coefficient α in terms of that for no saturation effects α_0 is given by[41]

$$\alpha = \frac{\alpha_0}{[(\nu-\nu_0)/\Delta\nu_0]^2 + 1 + P_{max}/(\Delta\nu)^2} \quad . \tag{21}$$

Similarly, the line width, $2\Delta\nu$, with saturation in terms of that without saturation, $2\Delta\nu_0$, is given by

$$2\Delta\nu = 2\Delta\nu_0\left[1+\frac{P_{max}}{(\Delta\nu_0)^2}\right]^{\frac{1}{2}} . \qquad (22)$$

Experimentally, saturation is often noticed when the power flux is as high as 1 milliwatt per square centimeter. In this investigation great care was taken to avoid saturation by carefully determining the power levels at which saturation becomes detectable; that power level was never exceeded during the course of the experiment. Thus, no corrections had to be made for saturation broadening.

Modulation Broadening

The microwave spectrograph used in this study uses frequency modulation of the source radiation in order to observe derivatives of the line shape. Application of a periodic sine or square wave modulation voltage of frequency f to the klystron results in the source radiation being modulated at the frequency f, with a frequency swing ("excursion") over one period that is dependent on the amplitude of the applied voltage. Line broadening due to modulation has been analyzed by Karplus[43] and experimentally verified by a number of investigators.[37]

Karplus's theory has been modified by Reinhart et al[44] for the case of "low-amplitude" modulation (as used in our spectrometer). In low-amplitude modulation the frequency excursion over one period of the modulation is less than

the half width. The correction that has to be applied to the second derivative profile to convert to the non-broadened line width is given by

$$\delta\nu = \Delta\nu\left[1+\frac{3}{16}\left(\frac{f'}{\Delta\nu}\right)^2+\frac{1}{2}\left(\frac{f}{\Delta\nu}\right)^2\right], \tag{23}$$

where f' is the frequency of the klystron over one period of the modulation, and f the modulation frequency (which was 17 KHz in these measurements).

Equation (23) was derived under the assumption of "slow-amplitude" modulation, i.e. $\frac{\Delta\nu}{2}>f$. For a modulation frequency of 17.0 KHz, this inequality is easily satisfied since measured line widths were usually in the range 50 — 200 KHz.

Equation (23) can be re-written as a quadratic equation in $\Delta\nu$, with roots determined by

$$\Delta\nu = \frac{1}{2}[\delta\nu\pm\{(\delta\nu)^2-(\frac{3}{4}f'^2+2f^2)\}^{\frac{1}{2}}] \ . \tag{24}$$

Only the positive root is retained in the above equation, otherwise $\Delta\nu=0$ for no modulation ($f'=f=0$). Using the positive root gives $\delta\nu=\Delta\nu$ for zero modulation (as is expected). Equation (23) therefore becomes

$$\Delta\nu = \frac{1}{2}\ \delta\nu+\{(\delta\nu)^2-(\frac{3}{4}f'^2+2f^2)\}^{\frac{1}{2}} \ . \tag{25}$$

Using the experimentally determined half widths $\delta\nu$ and f' as parameters, correction curves were calculated in order to obtain the non-modulated half width $\Delta\nu$. Figure 10 shows correction curves for several values of f', and over a wide range of $\delta\nu$ values.

In a series of measurements made by Rogers[45] (using the same spectrometer) it was found that f' was approximately 10.0 KHz. This low value for f' was achieved by setting the modulation voltage at about 50.0 mV. Care was taken in these measurements not to exceed this modulation voltage. From Figure 10, we observe that the correction $\delta\nu$-$\Delta\nu$ varies from about 5.0 KHz to about 2.0 KHz for measured line widths in the range 40.– 150. KHz. If the pressure change in this range of line widths is about 12.0 mTorr, the correction that has to be applied to the line width parameter $\Delta\nu_p$ is about 0.4 MHz/Torr. All our experimental line widths have been corrected for modulation broadening effects.

Overlapping Spectral Lines

It is occasionally observed that the frequency separation between the center frequency of separate transitions in a molecule is small enough to allow the absorption profiles of different lines to overlap when the lines are sufficiently broad (e.g., at high pressures). A line that is distorted by the presence of nearby lines is no longer characterized by a Lorentzian shape. The net result of such a distortion

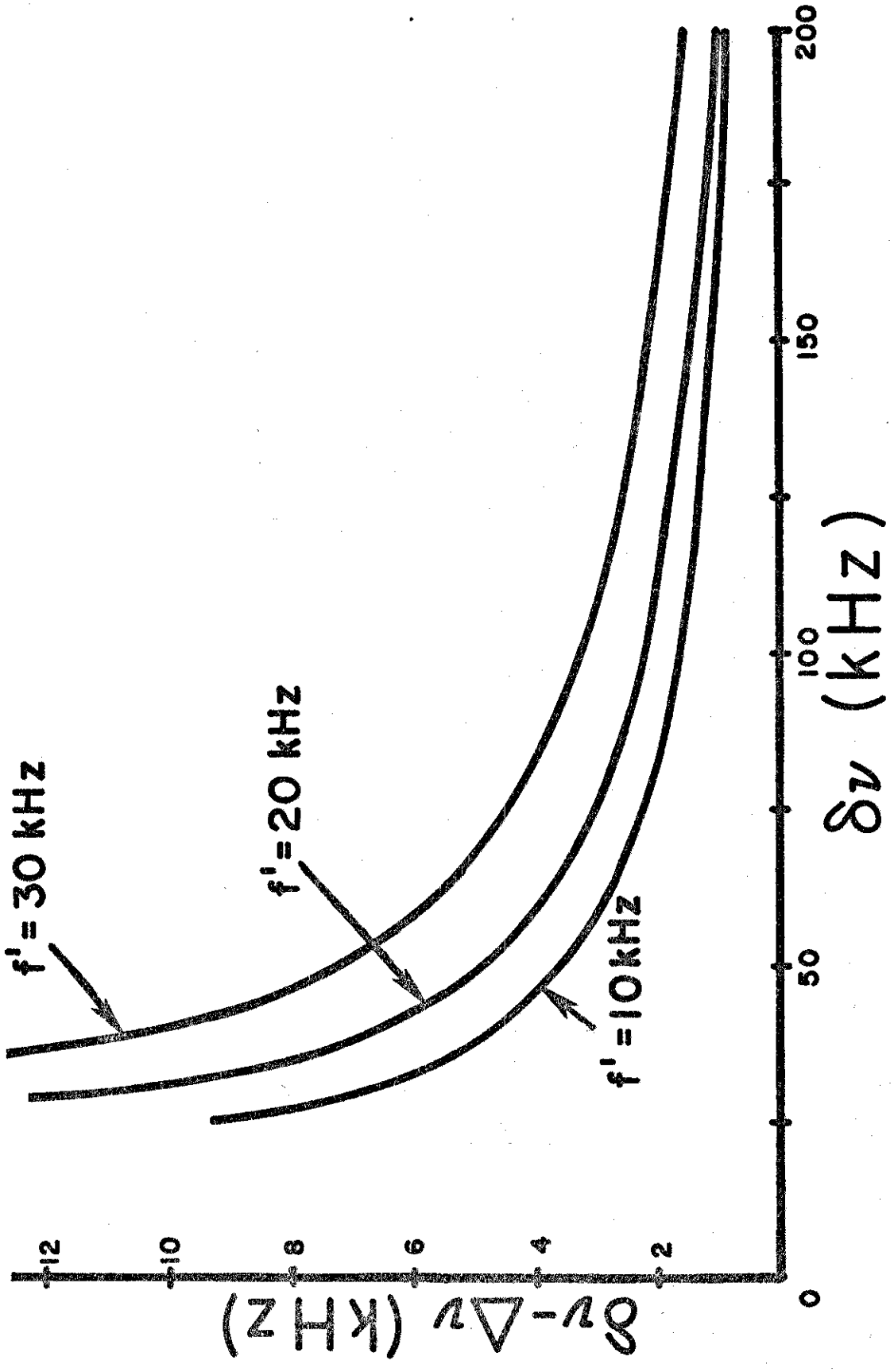

Fig. 10. Correction curves for modulation broadening; f = 17 kHz.

is a broadening of the given line. All the formaldehyde and formic acid lines studied in this investigation were quite narrow compared to the center frequencies of the individual rotational transitions. Therefore, no distortion due to overlap of spectral lines from separate rotational transitions was possible.

However, a problem similar to that discussed above arises in CH_2O and HCOOH due to the presence of magnetic hyperfine structure in these molecules. This magnetic hfs, proportional to $\vec{I}\cdot\vec{J}$, is due to the interaction of the magnetic moments of the nuclear protons with the magnetic field of molecular rotation.[46] Therefore, a rotational transition line observed in the laboratory for these molecules may actually be a composite of several hyperfine components. Figure 11 shows a typical hyperfine split line for CH_2O observed in this study. Similar hyperfine splitting was also observed for a number of formic acid lines. An analysis was undertaken to determine if the composite line was still Lorentzian in shape and a method has been worked out to correct for the presence of these hyperfine components. This analysis was necessary since corrections for Doppler and modulation broadening were made on the assumption that the observed line is Lorentzian.

The assumption is made that all the overlapping hyperfine components are Lorentzian in shape, have the same half

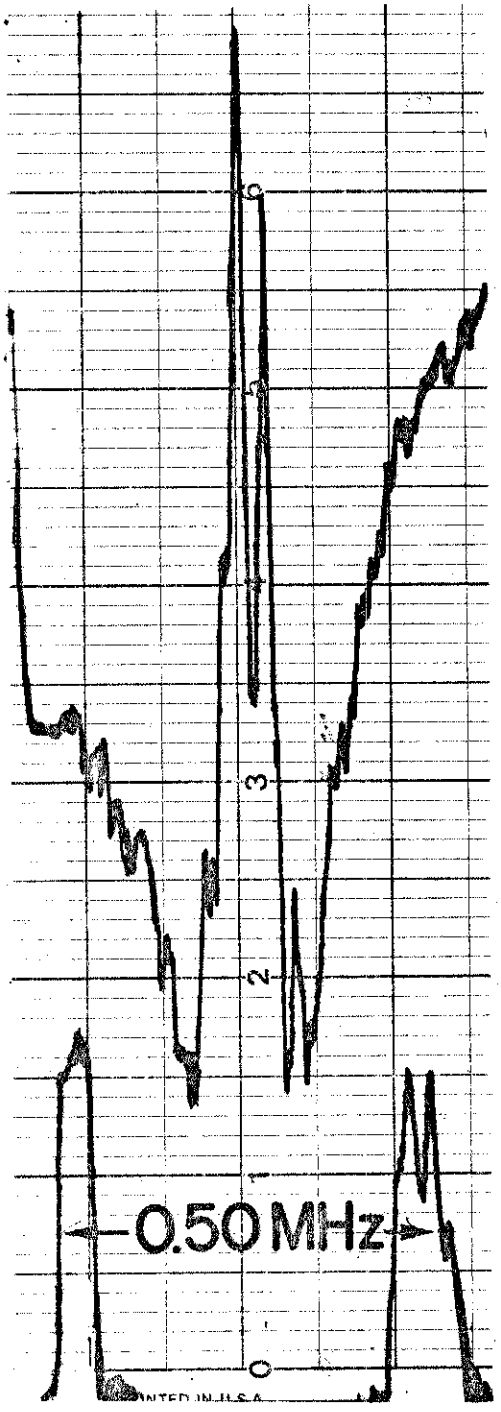

Fig. 11. Magnetic hfs for the $9_{2,8} \longrightarrow 9_{2,7}$ transition of CH_2O.

width, $\Delta\nu$, and that the envelope being measured is the resultant of these hyperfine spectral lines. An equation can be written for these lines as f(x), where f(x) is composed of the number of hyperfine lines which make up the envelope being measured. If the respective line intensities are I_j and the frequency spacings are a_j, then the equation for the composite spectra can be written as

$$\alpha = \sum_{j=1}^{n} I_j[(\nu-\nu_0+a_j)^2+(\Delta\nu)^2]^{-1} \equiv f(x) \quad . \tag{26}$$

For convenience in handling the above equation, the substitution $x=\nu-\nu_0$, which is the difference between the klystron frequency and a rather arbitrarily chosen "center" frequency for the system of lines, is made. The equation of f(x) is then

$$f(x) = \sum_{j=1}^{n} I_j[(x+a_j)^2+(\Delta\nu)^2]^{-1} \quad . \tag{27}$$

The peaks of the second derivative of f(x) are found by equating the third derivative of f(x) to zero; this gives

$$\sum_{j=1}^{n} I_j(x+a_j) \frac{(\Delta\nu)^2-(x+a_j)^2}{[(x+a_j)^2+(\Delta\nu)^2]^4} = 0 \quad . \tag{28}$$

Equation (28) can be solved numerically for the values of x that satisfy the requirement that the third derivative of f(x) is zero. The half width, $\Delta\nu$, is used as a parameter.

The frequency separation between the two outer peaks of the second derivative profile will then equal the value of $2\delta\nu$ observed experimentally for the unresolved envelope. However, before Equation (28) can be solved the intensities and the frequency spacing of each hyperfine component has to be known. Experimental data on these quantities is available for only a few CH_2O lines.[47,48] Magnetic hfs is such a small effect that it can only be fully resolved in beam maser spectrometry.[49] Unlike formaldehyde, no hyperfine splitting has yet been reported in the literature for formic acid. Published values[47] of I_j and a_j for five CH_2O transitions were used to obtain the curves shown in Figure 12. From these curves, it is evident that the dependence of $\delta\nu$ on $\Delta\nu$ is very nearly linear except for very narrow lines (i.e., at very low pressures). In fact, the ratio $\delta\nu/\Delta\nu$ is very nearly equal to one, indicating that the unresolved line broadens at the same rate as would a pure Lorentzian line.

An estimate for the error due to the presence of hfs can be made by examining Figure 12. Taking the $1_{11}\rightarrow 1_{10}$ transition as an example, the ratio $\delta\nu/\Delta\nu$ is found to be about 1.05. If the line width parameter $\Delta\nu_p$ is 20 MHz/Torr after making all other corrections, the true value of $\Delta\nu_p$ would be (20)(1.05)=21.0 MHz/Torr i.e. an increase of about 5%. Since only a few CH_2O lines could be precisely corrected for hfs, we estimate an error of about $\pm 2-5\%$ in the values

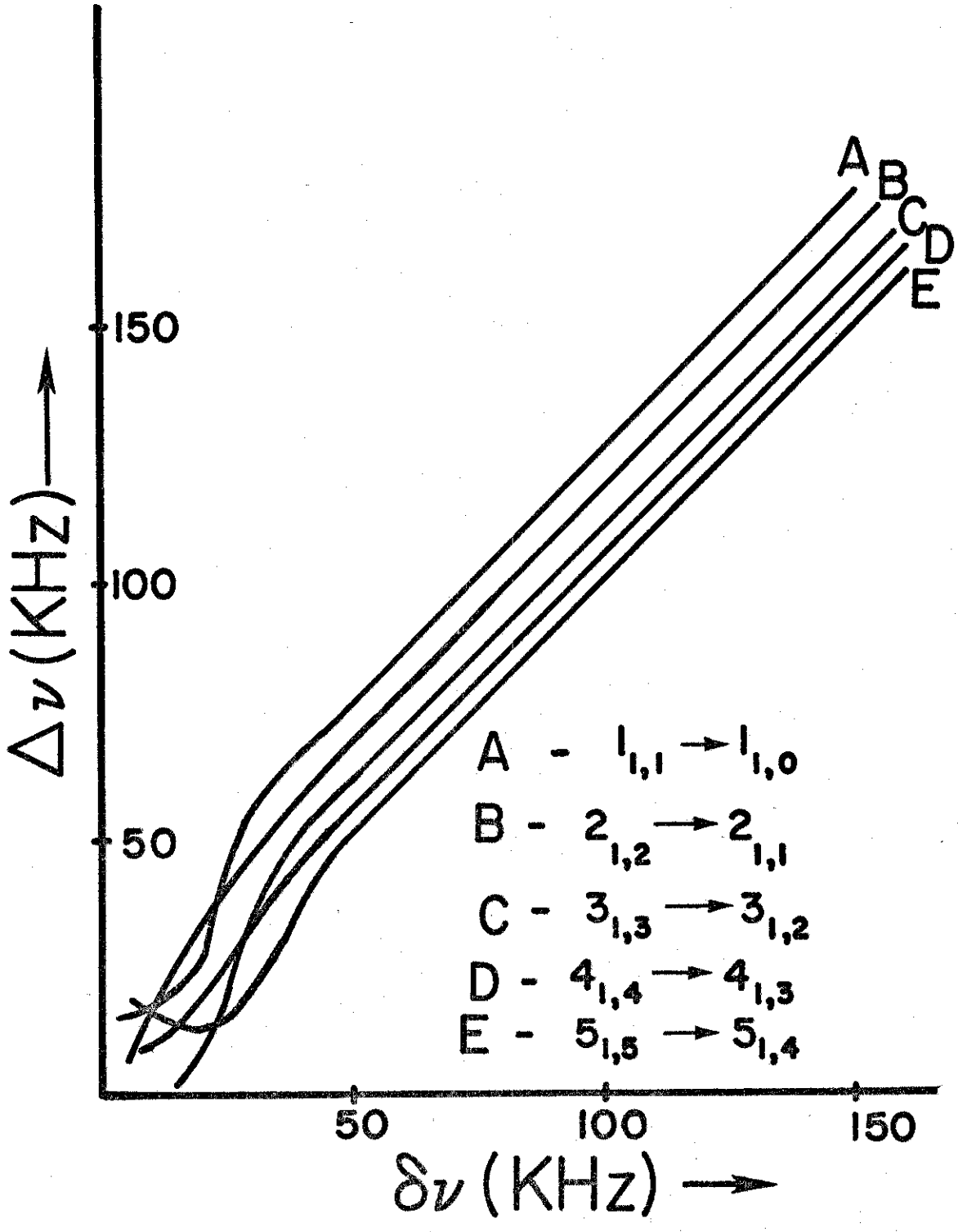

Fig. 12. Relation between $\delta\nu$ and $\Delta\nu$ for CH_2O lines with magnetic hfs.

of $\Delta\nu_p$ for lines which could not be corrected for the presence of hyperfine structure.

CHAPTER IV

PRESSURE BROADENING

The most important source of spectral line broadening in many microwave experiments is pressure broadening. It is also the most interesting because it provides information about how molecules behave in intermolecular collisions and hence about molecular force fields. This broadening arises as a result of collisions between molecules.

As mentioned in chapter III, the line widths of microwave spectra at low pressures can be adequately described by the concept that collisions initiate and terminate the molecular radiation or absorption. The Fourier analysis of the resulting wave trains gives a Lorentzian or resonance type variation in intensity of absorption with frequency[27] with the half-width $\Delta\nu$ of the absorption line related to the mean time τ between collisions by

$$\Delta\nu = \frac{1}{2\pi\tau} \quad . \tag{29}$$

Although the collision time is in general shorter than would be derived from kinetic theory cross sections, it is useful to define a cross section σ for microwave collisions by

$$\tau = \frac{1}{n\bar{v}\sigma} \tag{30}$$

where $\bar{v}$ is the relative velocity of impact and n the total number of molecules in the system. Combining Equations (30) and (31) gives

$$\Delta\nu = \frac{n\bar{v}\sigma}{2\pi} \quad . \tag{31}$$

Equation (31) reveals the linear relationship existing between the pressure broadened line width and pressure. The slope of the line obtained by plotting $\Delta\nu$ vs. pressure or the line width paramater, $\Delta\nu_p$, is then given by

$$\Delta\nu_p = \frac{\Delta(\Delta\nu)}{\Delta n} = \frac{\bar{v}\sigma}{2\pi} \quad . \tag{32}$$

Although the Van Vleck-Weiskoff theory correctly predicts the linear dependence of $\Delta\nu$ on pressure, the theory is incomplete since $\Delta\nu$ or $\Delta\nu_p$ is used as a parameter which has to be determined empirically. What is required is a theory which can correctly predict the value of $\Delta\nu$ at a given pressure, given certain information about the molecular properties (e.g., the dipole moment, quadrupole moment, etc). Experimentally measured $\Delta\nu$ or $\Delta\nu_p$ may then be interpreted in terms of intermolecular forces that arise during collisions.

Theories of Pressure Broadening

A complete treatment of pressure or collision broadening and evaluation of $\Delta\nu$ is so complex that a variety of treatments and approximations have been developed over the years. The various theories of pressure broadening can generally be classified into two categories: statistical and impact theories. The statistical theory developed by Kuhn and London[50] and Margeneau[51] assumes that molecules are always under the influence of intermolecular interactions, even though these may be weak, and that the frequency radiated depends on the amount of interaction occurring during radiation. The intensity radiated at a particular frequency ν depends simply on the probability that a molecule is perturbed by other molecules just the correct amount to make its frequency ν. Statistical theories hence always involve finding the probabilities of molecules being within a range R and R+ΔR apart with various possible angles of orientation and hence of their levels being perturbed by various amounts. Statistical theories cannot very well take into account the changes of interaction with time due to molecular motion and hence are good only when the molecular velocities are so low that the rate of change of intermolecular interactions may be neglected. This limitation prevents the statistical theory from being very accurate in the microwave region, although it has been used as a guide and rough approximation[52] for determining pressure broadened line widths.

On the other hand, impact theories assume that, during most of the time a molecule is sufficiently far from other molecules, it may be considered free. Occasionally, it comes close enough to one or more molecules for the intermolecular field to perturb its energy levels appreciably. After collision the molecule may be in the same state as before the encounter (i.e., an "adiabatic" collision), with only a change in phase of its wave function, or a transition to another state may have been induced by the collision (i.e., a "diabatic" collision). Both types of collisions contribute to pressure broadening. Since $kT>>h\nu$ for microwave frequencies, almost all collisions which are effective in broadening the spectral line are also strong enough to leave the molecule more or less in the upper or lower energy state. Therefore, diabatic collisions predominate in the microwave region.

Anderson[53] was the first one to propose a theory for pressure broadening due to diabatic collisions. His second-order perturbation treatment of pressure broadening is still the most frequently used method for analyzing intermolecular forces. However, Anderson's theory is very difficult to apply and does not work very well in many cases, frequently predicting values for $\Delta\nu_p$ which are too large.[54] Various modifications and extensions[55,56] to Anderson's theory exist in the literature and are frequently found to be easier to work with than the former (i.e., Anderson's treatment). Murphy and Boggs[54,57-60] have developed an alternative

formulation of the impact theory that works extremely well for pressure broadening of microwave spectral lines of linear and symmetric top molecules. However, the Murphy-Boggs theory often fails for asymmetric top molecules. For the sake of completeness, the basic assumptions of the impact theories and the results of the Anderson and Murphy-Boggs theories are given in the following sections.

Assumptions of Impact Theories

The basic assumptions common to all impact theories are: (1) the "impact approximation," (2) the "assumption of a classical path," and (3) all spectral lines are well resolved.

In the impact approximation, it is assumed that (a) the duration of a collision is small compared to the mean time between collisions, and (b) the collisions are binary. Both these assumptions are valid at low pressures.[61]

The assumption of classical paths is equivalent to assuming that the molecules are point dipoles that follow definite classical paths. In very close collisions this is a poor assumption, but the errors introduced are unimportant since any path giving a close collision involves complete interruption of the radiation, and details of the paths are unnecessary. Collisions near the limit of the effective collision radius are the ones which must be accurately treated, and the quantum-mechanical wave packet for each molecule

may in almost all cases be considered sufficiently small compared with this distance to make the classical path a very good assumption.

The third and final assumption is that all microwave spectral lines are well resolved. Although this is not quite true for the spectral lines of CH_2O and HCOOH which have fine structure (as discussed in Chapter III), Anderson has shown that if the lines are not resolved at all compared to the line width, the separate components may be treated as degenerate.

The general procedure in impact theories is to make use of these assumptions and knowledge of the rotational energy levels to calculate the probability that various types of collisions occur. Disturbances of molecular radiation (phase shifts and transitions) are accounted for in each type of collision. Then a Fourier analysis is performed to determine the distribution of the spectral intensity as a function of frequency.

Anderson's Theory

Using the assumptions discussed in the preceding section, Anderson has obtained a line shape for microwave spectral lines similar to that of Van Vleck and Weiskoff [Equation (2)] with the possibility of a shift in the center frequency

$$\alpha(\nu) = \frac{8\pi^2 Nf}{3ckT} |\mu_{ij}|^2 \nu^2 \Delta\nu\{(\nu-\nu_0-a\Delta\nu)^2+(\Delta\nu)^2\}^{-1} . \qquad (33)$$

The pressure-induced shifts in center frequencies is given by $a\Delta\nu$, where a is a constant and $\Delta\nu$ the half width. These shifts are very small for microwave lines and only a few are reported in the literature.[62] Anderson's expressions for the line widths and frequency shifts, in mixtures of two different types of molecules (denoted by the subscript 1 and 2), where the number of molecules per unit volume is n_1 and n_2, respectively, may be written as

$$2\pi\Delta\nu = n_1\bar{v}_{11}\sigma'_{11} + n_2\bar{v}_{12}\sigma'_{12} \tag{34}$$

$$2\pi\Delta\nu_0 = n_1\bar{v}_{11}\sigma''_{11} + n_2\bar{v}_{12}\sigma''_{12} \quad . \tag{35}$$

Subscript 1 refers to the molecule ("absorber") whose line is being observed, and subscript 2 applies to the other type of molecule ("perturber") involved in the binary collisions. The symbol $\bar{v}$ refers to the mean relative velocity between the molecules, and σ' and σ'' are the real and imaginary parts of the collision cross sections, respectively. Note that when $n_2=0$, i.e., for self broadening, Equation (34) reduces to Equation (31) obtained from the Van Vleck-Weiskoff theory.

In Anderson's theory the total collision cross section σ is defined as

$$\sigma = \sigma'+i\sigma'' = \int_0^\infty 2\pi bS(b)db \ , \tag{36}$$

where b is the impact parameter, or distance of closest

approach of the colliding molecules, so that $2\pi b\ db$ is proportional to the probability of a collision with impact parameter b, and S(b) is a weight factor which indicates whether or not a collision is effective in disturbing the process of molecular radiation. The impact parameter b is defined by the equation

$$r^2 = b^2+v^2t^2 \ , \tag{37}$$

with the physical picture of the binary collision being represented by Figure 13.

Anderson has shown that as a first approximation[53] it is possible to write the weight factor, S(b), as a combination of two terms

$$S(b) = S_1(b)+S_2(b) \ , \tag{38}$$

where $S_1(b)$ is imaginary and may be defined as the weight factor for collisions which are responsible for causing frequency shifts, and $S_2(b)$ is the weight factor for collisions causing line broadening. The behavior of $S_2(b)$ as a function of the impact parameter b is shown in Figure 14. Using Equation (38) and the fact that for $0 \leq b \leq b_0$, $S_2(b)=1$, the collision cross section for line broadening may be written as

$$\sigma' = \pi b_0^{\,2} + \int_{b_0}^{\infty} 2\pi S_2(b)\ b\ db \ , \tag{39}$$

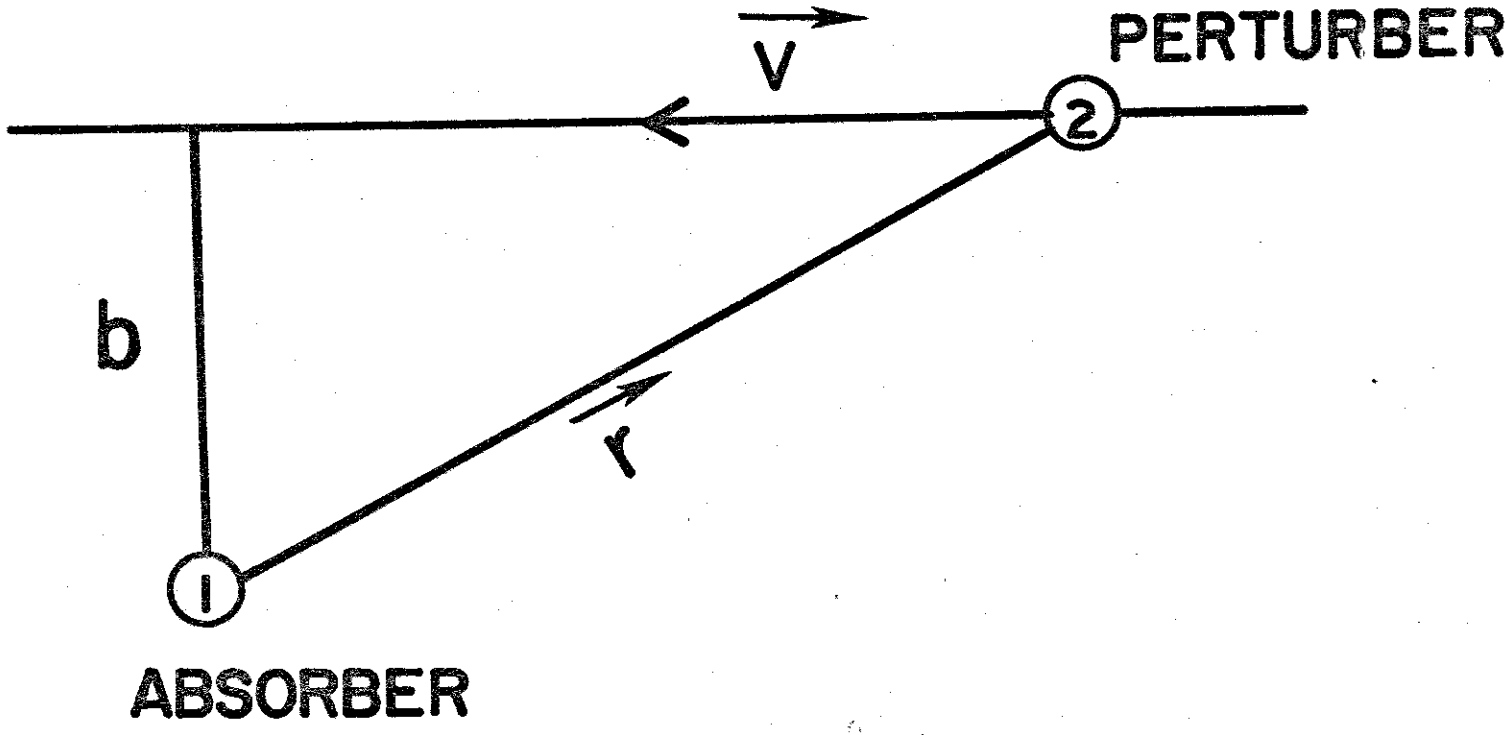

Fig. 13. Geometry of a binary molecular collision.

with b_0 determined by the condition

$$S_2(b_0) = 1 \ . \tag{40}$$

Expressions for $S_2(b)$ for various interactions are available in the literature. In particular, the expressions derived by Birnbaum[63] for dipole-quadrupole interactions, and dipole-induced dipole interactions have been utilized to calculate cross sections for collisions between HCOOH (and CH_2O) and foreign gases (H_2 and He). The results of these calculations are discussed in Chapter VI.

Murphy and Boggs Theory

Murphy and Boggs[54] have developed a theory of pressure broadening in which the line width is computed using the relation

$$\Delta\nu = \frac{1}{4\pi\tau_i} + \frac{1}{4\pi\tau_f} \ , \tag{41}$$

where τ_i and τ_f are, respectively, the average lifetimes of the initial and final rotational energy levels of the radiating molecule. By neglecting the effects of phase shifts on the line width and ignoring the probability of the molecule making a transition back to the original level once it has left, that is $J' \neq J$, they obtained for the lifetime of state J_1

$$\frac{1}{\tau_{J_1}} = \Sigma \rho_{J_2} \Phi(J_1 J_2) \quad , \tag{42}$$

where ρ_{J_2} is the relative population of the rotational state J_2, and $\Phi(J_1 J_2)$ is the number of transitions per unit time out of the J_1 energy level caused by collisions with molecules in the J_2 levels and is written explicitly as

$$\Phi(J_1 J_2) = 2\pi N \int_0^\infty b db \int_0^\infty v dv F(v) \{1 - \exp[-\Gamma_{J_1 J_2}(b,v)]\} \quad , \tag{43}$$

where N is the number of molecules per unit volume, F(v) is the Maxwell-Boltzmann velocity distribution function, and b is the impact parameter. The quantity $\Gamma_{J_1 J_2}(b,v)$ evaluated on the basis of the straight line path approximation and a perturbation expansion of the interaction matrix,[54] is given by

$$\Gamma_{J_1 J_2}(b,v) = 2 S_2(b)_{0,1} \quad , \tag{44}$$

where $S_2(b)_{0,1}$ is Anderson's weight factor with the term $J_1' = J_1$ omitted.

The most important difference in the two theories discussed in this chapter is the average of the $S_2(b)$ function over the impact parameter b. Anderson first normalized $S_2(b)$ for the value of b (say b_0) then integrated over b from b_0 to ∞ [Equation (39)]. On the other hand Murphy and Boggs evaluated the double integral of the function $\Gamma(b,v)$ by means of a 15-point Gauss-Laguerre quadrature procedure. This

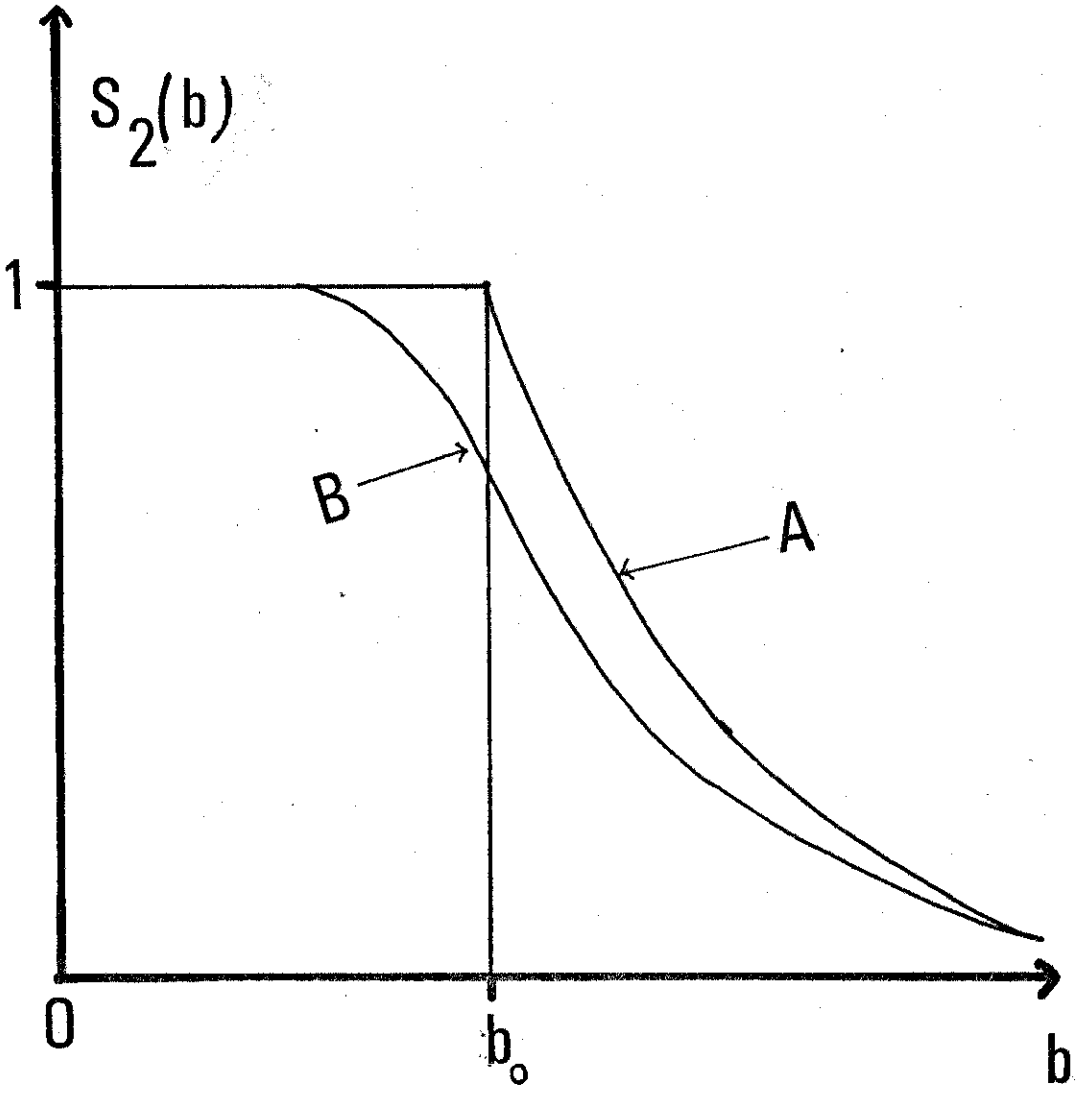

Fig. 14. Graph of $S(b_2)$ for the two impact theories summarized in this chapter. (A) Anderson theory; (B) Murphy-Boggs theory.

difference can be seen in Figure 14. Because of this difference in weight factors the line widths calculated using the theory of Murphy and Boggs are generally smaller than those calculated by Anderson's theory.

CHAPTER V

INSTRUMENTATION

One of the most important phases of microwave line width spectroscopy is the instrumentation needed to produce a dependable spectrograph that can be used to obtain reliable data. Such an instrument has to be capable of measuring small frequency intervals accurately. A number of low-pressures spectral lines of CH_2O and HCOOH have line widths on the order of 40.0 – 60.0 KHz, so frequency differences must be measurable to a few kilohertz.

A block diagram of the line width spectrograph used in this investigation is shown in Figure 15. This spectrograph has been discussed in detail by Roberts[64] and Rogers.[20,45] For the sake of convenience, the spectrograph is divided into five main sections: (1) the radiation source (klystron) and associated electronics, (2) the absorption cell, (3) signal detection, amplification, and display, (4) frequency measuring system, and (5) vacuum and gas handling system. Each section will be discussed separately in this chapter.

Microwave Source and Controls

Reflex klystrons manufactured by OKI and Varian were utilized as sources of microwave radiation in this spectrograph. These klystrons produced fundamental frequencies at

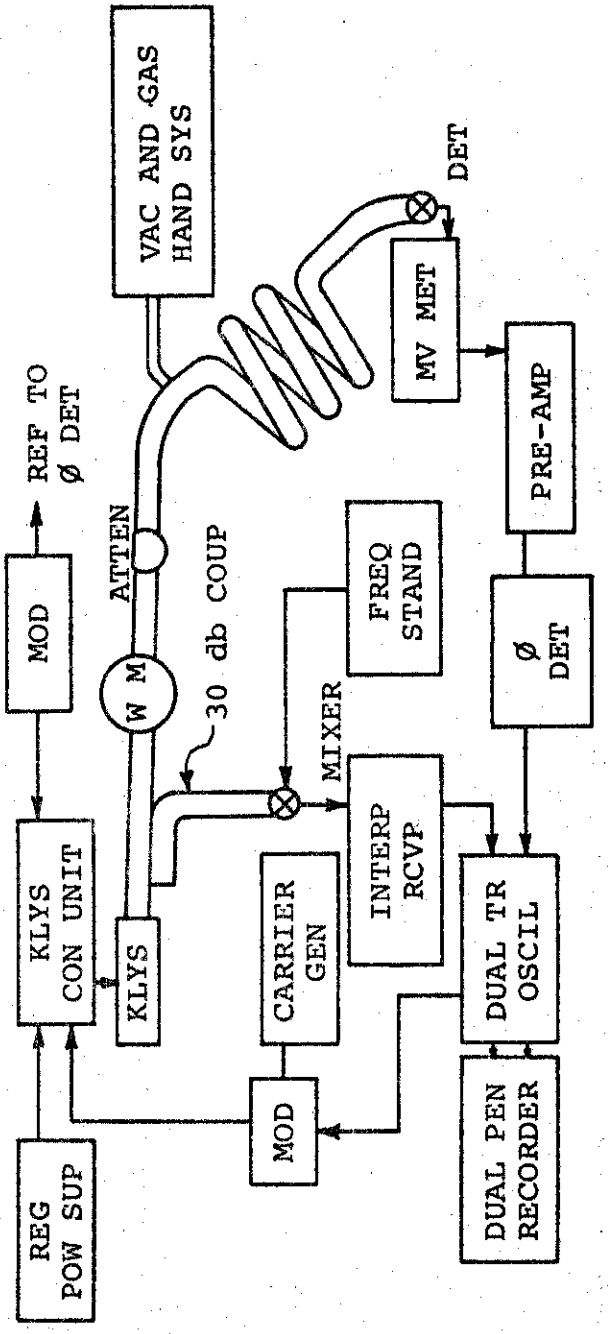

Fig. 15. Block diagram of line width spectrograph.

the desired CH_2O and HCOOH transition frequencies; some higher frequencies could only be reached by frequency doubling in crystal harmonic generators. This is a common technique, and adequate power is available at the first harmonic; but occasionally spurious modes are generated, so that this method was avoided whenever possible

Coarse frequency tuning of the klystron is performed by mechanically adjusting the cavity size with a tuning stub attached to the cavity. Fine tuning (over a range of several MHz) is accomplished by varying the focus and repeller voltages. In order to minimize source broadening the klystron was submerged in an oil bath to reduce instabilities due to mechanical vibrations and thermal gradients.

Two power supplies were used in the spectrograph. They were a Hamner Model N-4035 high-voltage supply (maximum voltage 3600 V) and an Electronic Measurements Model C612 constant current supply (voltages to 300 V). The Hamner supply must be used for OKI klystrons as these require negative repeller voltages of the order of 2000 V.

The klystron control unit (Figure 15) is designed so that the focus, anode (beam), and reflector potentials may be conveniently adjusted. Fine adjustments are necessary to properly bias the klystron into oscillation and also for fine tuning of the source frequency. In addition, the control unit has special provisions for applying source modulation and oscilloscope sweep voltages to the klystron repeller.

Modulation of the repeller by a square or sine wave voltage is a feature of "source modulation" spectrographs, and serves to modulate the output frequency so as to permit narrow-band ac amplification and phase sensitive detection of the absorption signal (the source frequency is modulated, not the source power). The required klystron modulation was provided by a slow sweep sawtooth signal generated by the horizontal sweep of the time base generator of the oscilloscope upon which was superimposed a sine wave signal generated by a Heath Company Model EUW 27 Sine-Square wave generator. Sine wave modulation was used in order to experimentally detect the second derivative of the resonance profile.

Absorption Cell

Two types of absorption cells were used in this investigation. These were, a copper cell of circular cross-section, with an inside diameter of 5 cm, and a rectangular aluminum cell with dimensions 1.8 cm and 2.5 cm respectively. Both these cells were coiled with a mean coil diameter of about 1 meter to conserve space and to place the source and detector ends close together. The ends of the cells were vacuum sealed with Teflon plates that were approximately 7 mm thick. The dimensions of the cells were so chosen that the cut-off frequencies of the propogating waves in these cells are far lower than the transition frequencies of most of the known CH_2O and HCOOH lines.

An important factor concerning the cell is its length. Townes and Schawlow[65] have shown that the optimum cell length is given by the expression $L=2/a_0$, where a is the attenuation constant. The value of a_0 is typically of the order $10^{-3}\,cm^{-1}$, the "best" length would be in the range 5 to 30 m. The length of both the above mentioned cells is about 12 m, thereby meeting the criterion of an ideal absorption cell.

Signal Detection, Amplification, and Display

Power absorption due to microwave transitions in a gaseous sample is often less than $1/10^6$ of the off-resonance power level in the cell, and it is these small power absorptions that must be measured to obtain accurate line widths. This makes the detection and amplification of the signal an extremely critical stage of the experimental process. Detection of the microwave power absorption was achieved by the standard method of crystal rectification. Crystal diodes used were generally 1N26 silicon type, with 1N23 diodes employed for frequencies below 12 GHz.

Voltage signals from the crystal detector (5-20 mV) were first amplified in a high-gain transistor pre-amplifier, designed and constructed in the department electronics shop. A detailed discussion of this pre-amplifier is given by Rogers.[45] After the signal was amplified in the pre-amplifier it was sent to a PAR Model 122 phase-sensitive detector.

Sensitivity settings of 50 and 20 mV were typically used in these experiments.

Visual display of the phase detector output signal was provided by using the Tektronix 502 A dual-trace oscilloscope. The phase detector signal was also sent to one pen of a dual-channel Rikadenki B-261 strip chart recorder for a permanent record of the data. Figure 11 shows a typical recorder display of a second derivative profile of a spectral line.

There are four main reasons for experimentally observing derivatives of the line instead of the absorption profile. First, modulating the klystron output frequency permits use of high-gain ac amplification. Second, base line noise makes precise detection of the half-power points very difficult, whereas the inflection points of the derivatives are easy to locate. Third, distortions due to standing waves are reduced by using derivatives. Finally, frequency resolution was improved by observing second derivatives. The overall frequency resolution of this spectrograph is found to be about 20 KHz based on measurements on partially resolved magnetic hfs of CH_2O and HCOOH (Figure 11).

Frequency Measurements

The small frequency intervals that have to be determined in line width measurements can be obtained by producing "frequency markers" of known frequency on the same chart

that records the derivative of the line shape. The half power half-widths can then be determined by using the marker separation as a frequency basis.

The markers were generated by mixing part of the source radiation (extracted with a 30-db coupler) with radiation from a Hewlett-Packard Model 612A UHF signal generator. Sum and difference frequencies were obtained by crystal-mixing the two signals; the difference frequencies were in the radio-frequency range, and were detected with a Wells-Gardner Model BC-348Q radio receiver. The receiver was typically tuned to receive 250 KHz difference frequencies. The net result is the appearance of two frequency markers at intervals ±250 KHz from the line center. The visual display of these markers is shown in Figure 11. The total separation of 500 KHz is used as a basis for measuring the line width.

Vacuum and Gas Handling Systems

Evacuation of the absorption cell was carried out by using LN_2 cold-trapped Van Waters and Rogers HV-1 oil-vapor diffusion pump connected to a Welch Duo-seal Model 1405 forepump. Pressures within the cell were measured with a Hastings gauge that had been calibrated against a standard McLeod gauge. The McLeod gauge was not suitable for pressure measurements on CH_2O and HCOOH as these gases could not withstand the compression in the gauge chambers above a few microns of pressure. The Hastings gauge proved to be quite

satisfactory as a secondary standard after calibration. Calibration of the Hastings gauge was carried out by adjusting the Hg level in the capilliary of the McLeod gauge to as small a compression ratio as could be tolerated and still obtain reasonable height readings.

Graphs of the Hastings gauge readings versus the corresponding McLeod gauge readings were used to determine calibration constants for the Hastings gauge (it is assumed that the McLeod gauge gives the correct pressure reading). Linear least square fits were then performed on the data points to obtain the calibration factors. The Hastings gauge readings have to be multiplied by the following factors to get the true pressures: $CH_2O - 0.725$, $HCOOH - 0.61$, $H_2 - 0.639$, and $He - 1.14$.

Gases were admitted into the cell from a series of "dosing" reservoirs. Four such reservoirs were used, one each for the above mentioned gases. The He and H_2 used in these investigations were high purity samples obtained from Union Carbide Company. The formic acid used was purchased from Eastman Kodak Company and was 99.5 per cent pure.

The gas CH_2O used in this investigation was prepared by evacuating the space above a sample of pure paraformaldehyde. When all the residual gases had been pumped off, the sample was gently heated to release CH_2O of about 95 per cent purity.[7] The main impurity in the vapor of formaldehyde

is water which was removed by passing CH_2O through a P_2O_5 trap. The pure gas (99.7 per cent pure) was then pumped into the dosing reservoir for storage.

Temperature Studies on CH_2O Lines

Temperature studies on the self-broadening of CH_2O for the $3_{1,3} \longrightarrow 3_{1,2}$ and $17_{3,15} \longrightarrow 17_{3,14}$ transitions were carried out by heating the absorption cell by high-intensity lamps mounted on top of the cell. The cell was contained in a thermal jacket made of an insulating material. The cell was heated for 6-8 hours prior to each line width parameter measurement. After the gas was introduced into the cell, it was allowed sufficient time to acquire the temperature of the cell and stabilize itself. The line width was then measured. The corresponding pressure of the gas was also corrected for increase in temperatures by using the ideal gas law. The temperature of the cell was measured by using five Fe-Cu thermocouples mounted in series (i.e., a thermopile) with each junction placed at different points along the cell. The accuracy of these temperature measurements is about $\pm 0.5°C$.

CHAPTER VI

EXPERIMENTAL RESULTS AND ANALYSIS

The experimentally measured line width parameters $\Delta\nu_p$ for both self broadening and foreign-gas (H_2 and He) broadening of the rotational lines of formic acid and formaldehyde are shown in Tables I and II respectively. All transitions studied in the investigation were of the type $\Delta J=0$ (i.e., Q-branch transitions), with $\Delta K_-=0$ and $\Delta K_+=+1$. J is the total angular momentum quantum number of the rotational state, K_- is the projection of J on the symmetry axis of a limiting prolate top, and K_+ is the projection of J on the symmetry axis of a limiting oblate top. The rotational energy levels of asymmetric top molecules like CH_2O and HCOOH are normally labelled by the notation $J_{K_-K_+}$ or J_τ, where $\tau=K_--K_+$. The arrows between the states (as shown in Tables I and II) indicate the direction of transition for absorption. Some of the low-lying rotational energy levels for HCOOH and CH_2O are shown in Figures 16 and 17 respectively.

All measurements listed in Tables I and II were made at 300°K on binary gas mixtures using the spectrometer described in Chapter VI. All experimentally determined line widths $\Delta\nu$ were corrected for broadening due to Doppler and Modulation effects. As stated in Chapter III, no corrections had to be

TABLE I

EXPERIMENTAL VALUES OF LINE WIDTH PARAMETERS AND COLLISION DIAMETERS FOR THE HCOOH MOLECULE

Transition	Frequency (MHz)	$\Delta\nu_p$ (MHz/Torr)			Collision Diam. (Å)		
		HCOOH	H_2	He	HCOOH	H_2	He
$3_{1,3} \rightarrow 3_{1,2}$	9831.98	12.31	5.41	2.37	12.10	4.31	3.34
$6_{1,6} \rightarrow 6_{1,5}$	34378.88	12.25	6.10	2.50	12.07	4.58	3.43
$9_{2,8} \rightarrow 9_{2,7}$	9696.83	12.63	4.68	1.85	12.25	4.01	2.95
$11_{2,10} \rightarrow 11_{2,9}$	20297.88	12.31	5.14	3.08	12.10	4.20	3.81
$12_{2,11} \rightarrow 12_{2,10}$	27758.05	12.23	5.40	2.78	12.06	4.30	3.61
$16_{3,14} \rightarrow 16_{3,13}$	8968.50	9.85	5.30	2.25	10.82	4.27	3.25
$20_{3,18} \rightarrow 20_{3,17}$	30523.12	9.30	4.8	2.25	10.52	4.1	3.25
$24_{4,21} \rightarrow 24_{4,20}$	9410.00	9.10	4.59	1.70	10.41	3.97	2.83
$28_{4,25} \rightarrow 28_{4,24}$	28935.00	9.98	5.40	2.40	10.90	4.30	3.36
$32_{5,28} \rightarrow 32_{5,27}$	8662.00	12.01	5.8	2.56	11.95	4.4	3.47

TABLE II

EXPERIMENTAL VALUES OF LINE WIDTH PARAMETER AND COLLISION DIAMETERS FOR THE HCHO MOLECULE

Transition	Frequency (MHz)	$\Delta\nu_p$ MHz/Torr			Collision Diam. (Å)		
		HCHO	H_2	He	HCHO	H_2	He
$7_{2,6} \rightarrow 7_{2,5}$	8884.87	20.7	6.52	3.1	14.1	4.71	3.8
$9_{2,8} \rightarrow 9_{2,7}$	22965.71	19.0	7.72	2.96	13.51	5.12	3.7
$11_{2,10} \rightarrow 11_{2,9}$	48612.70	26.2	9.55	3.25	15.9	5.7	3.9
$15_{3,13} \rightarrow 15_{3,12}$	11753.13	22.0(a) 7.7(b)	3.0(a) 0.35(b)	1.9	14.5(a) 8.6(b)	3.18(a) 1.1(b)	2.96
$17_{3,15} \rightarrow 17_{3,14}$	24068.31	24.96(a) 12.44(b)	8.5(a) 3.15(b)	4.49(a) 1.56(b)	15.48(a) 10.93(b)	5.37(a) 3.27(b)	4.55(a) 2.69(b)
$19_{3,17} \rightarrow 19_{3,16}$	45063.	14.22(a) 10.0(b)	5.70	3.70	11.70(a) 9.80(b)	4.4	4.10
$25_{4,22} \rightarrow 25_{4,21}$	19595.23	15.33(a) 2.51(b)	4.91	1.22	12.13(a) 4.91(b)	4.08	2.4

Note: (a) and (b) refer to the two slope parameters with a knee observed in $\Delta\nu_p$.

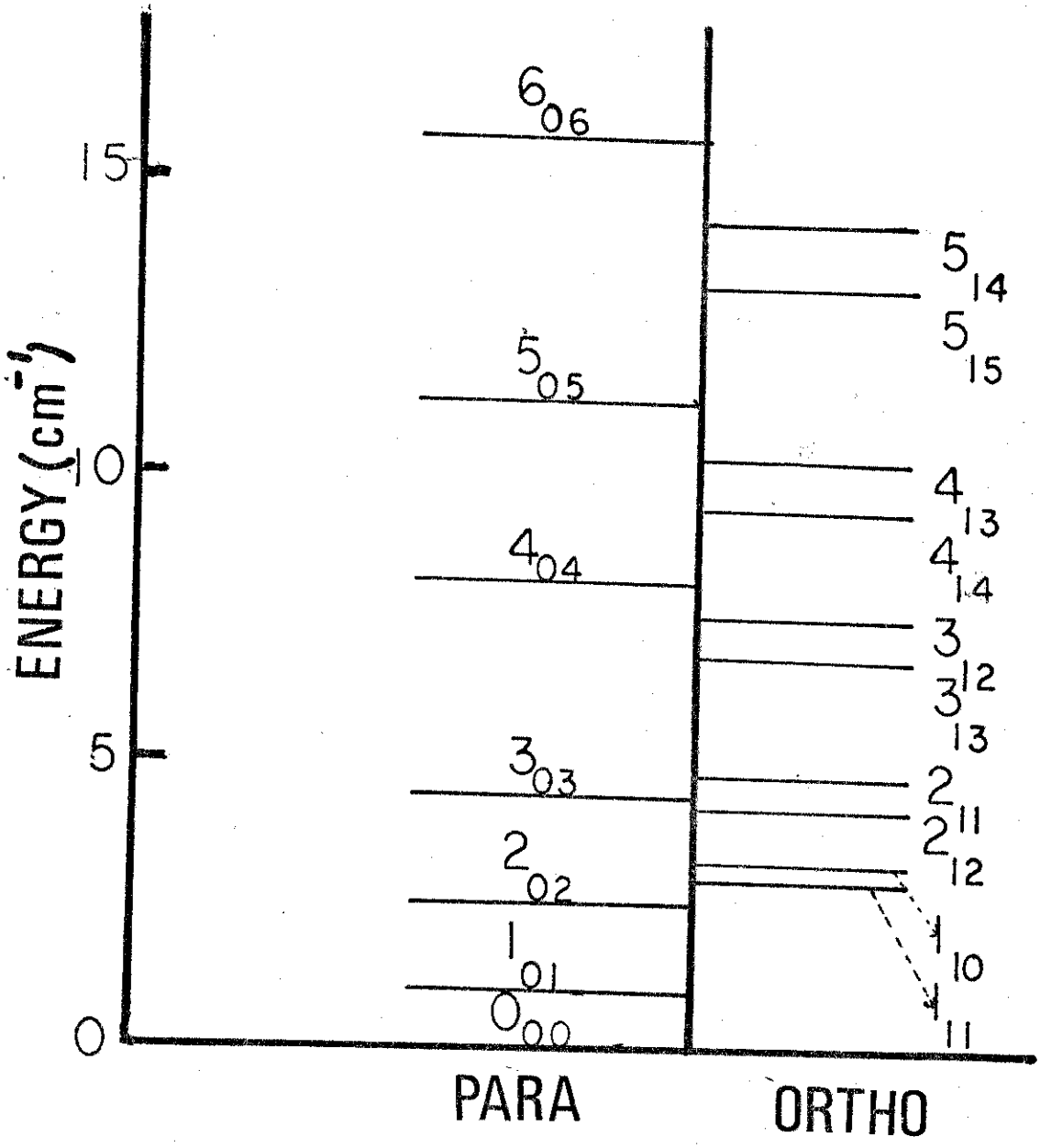

Fig. 16. Low energy levels of formic acid.

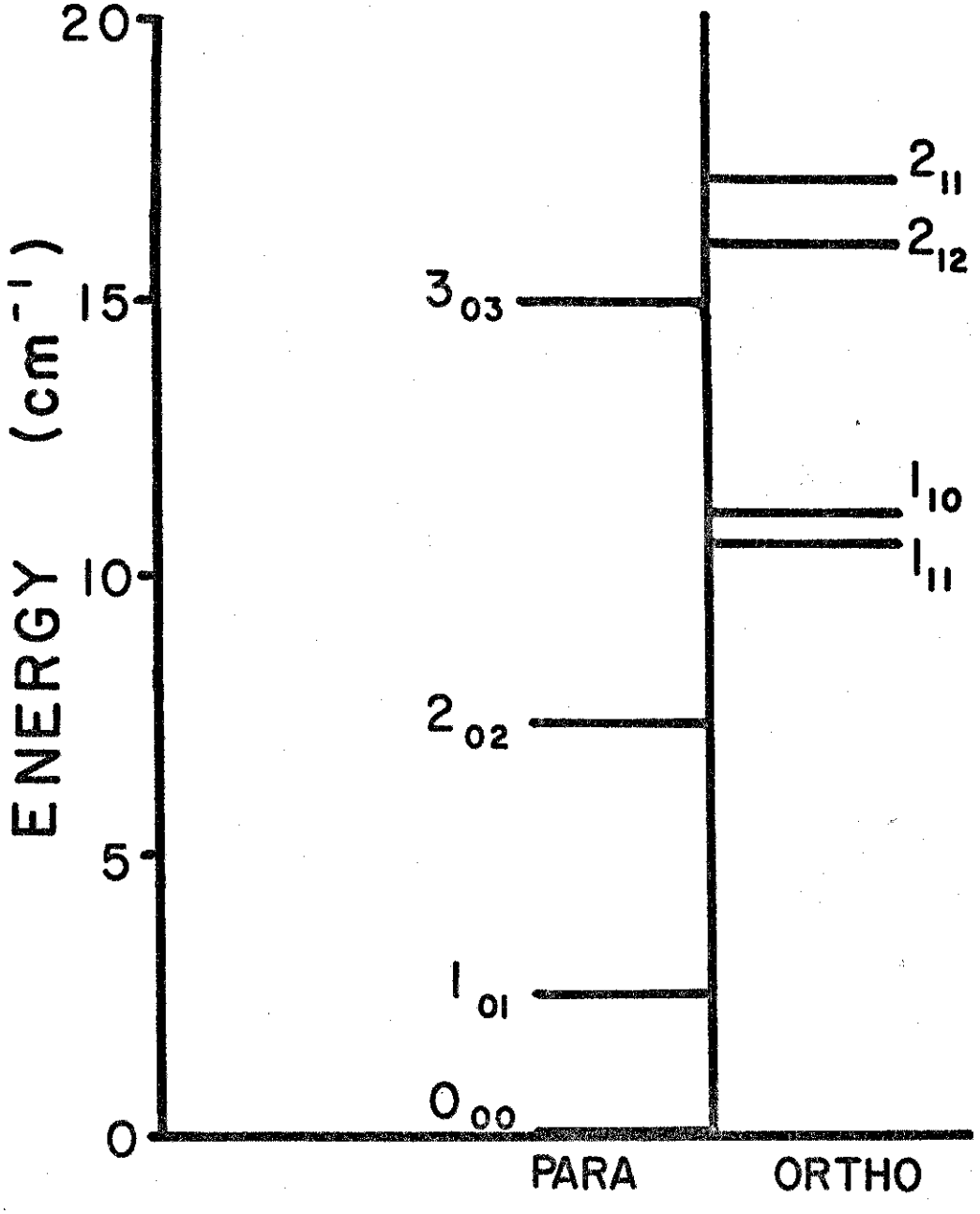

Fig. 17. Low energy levels of formaldehyde.

made for broadening due to saturation effects, collisions with the cell walls, etc., as their contribution to the line width is negligible. Values for the line width parameters $\Delta\nu_p$ for the various gaseous mixtures were determined by plotting the corrected line widths $\Delta\nu$ vs. pressure, and performing a linear least square fit on the data points. Figure 18 shows a typical line width parameter curve obtained in this investigation. For a number of CH_2O lines, it was found that the best fit to data points could only be obtained by using two pressure ranges and employing two linear least square fits (see Figure 19). We have statistically examined the possibility of other fits such as a single line or curve; however, all other fits result in a much greater departure from the data points than that obtained by using a two range linear fit. In those transitions of CH_2O, which produced two distinct line width parameters, both are reported in Table II.

The collision diameters listed in Tables I and II for the interactions HCOOH-HCOOH, CH_2O-CH_2O, HCOOH-H_2, CH_2O-H_2, HCOOH-He, and CH_2O-He are equivalent hard sphere diameters calculated from the experimental values of $\Delta\nu_p$ with the aid of the equations[66]

$$b_1 = (\alpha)^{\frac{1}{2}}(M_1 \pi kT/4N_0)^{\frac{1}{4}} \tag{45}$$

$$b_2 = (\beta)^{\frac{1}{2}}(M_2 \pi kT/2N_0)^{\frac{1}{4}} \, . \tag{46}$$

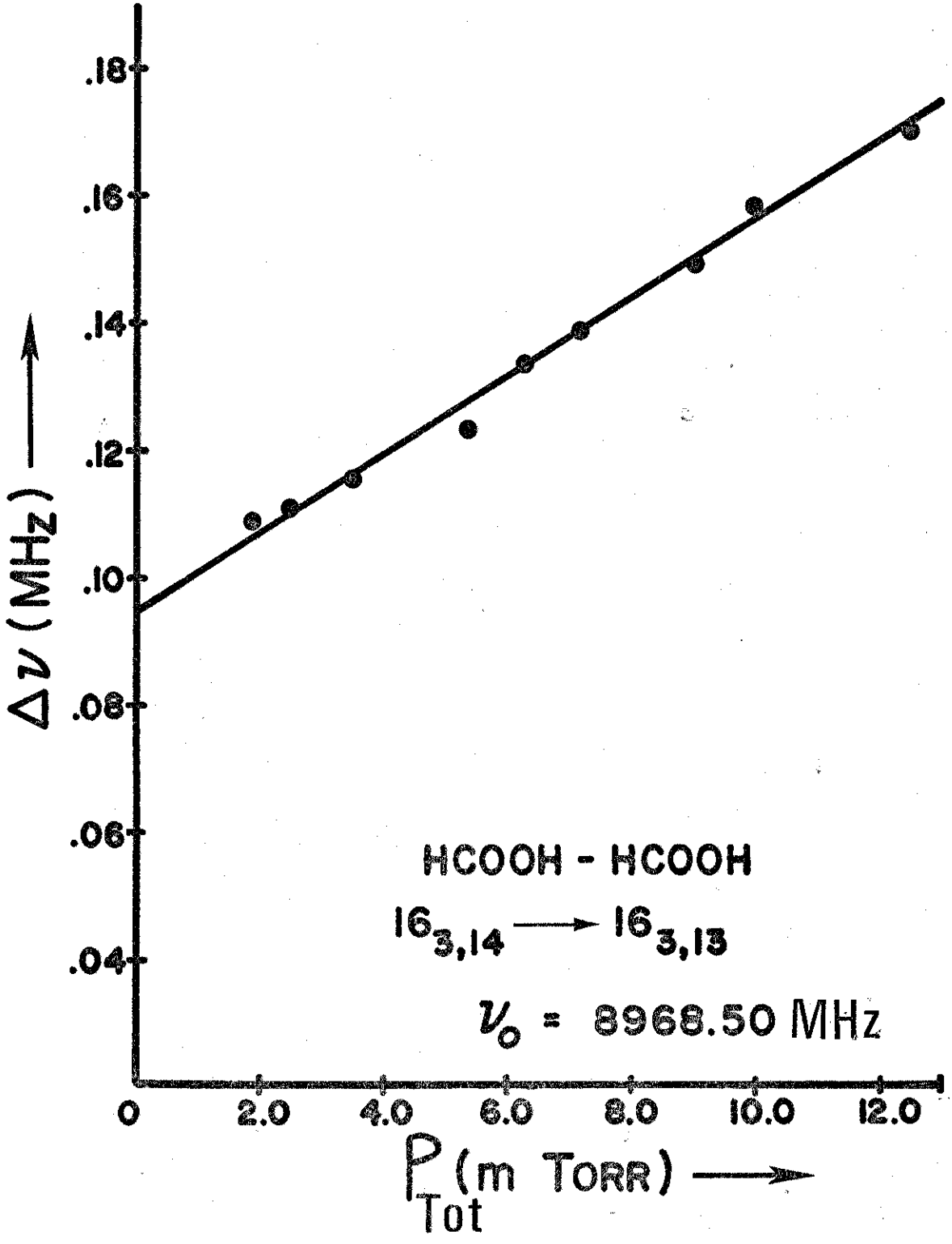

Fig. 18. Line width parameter curve for deducing collision diameters in HCOOH-HCOOH mixtures.

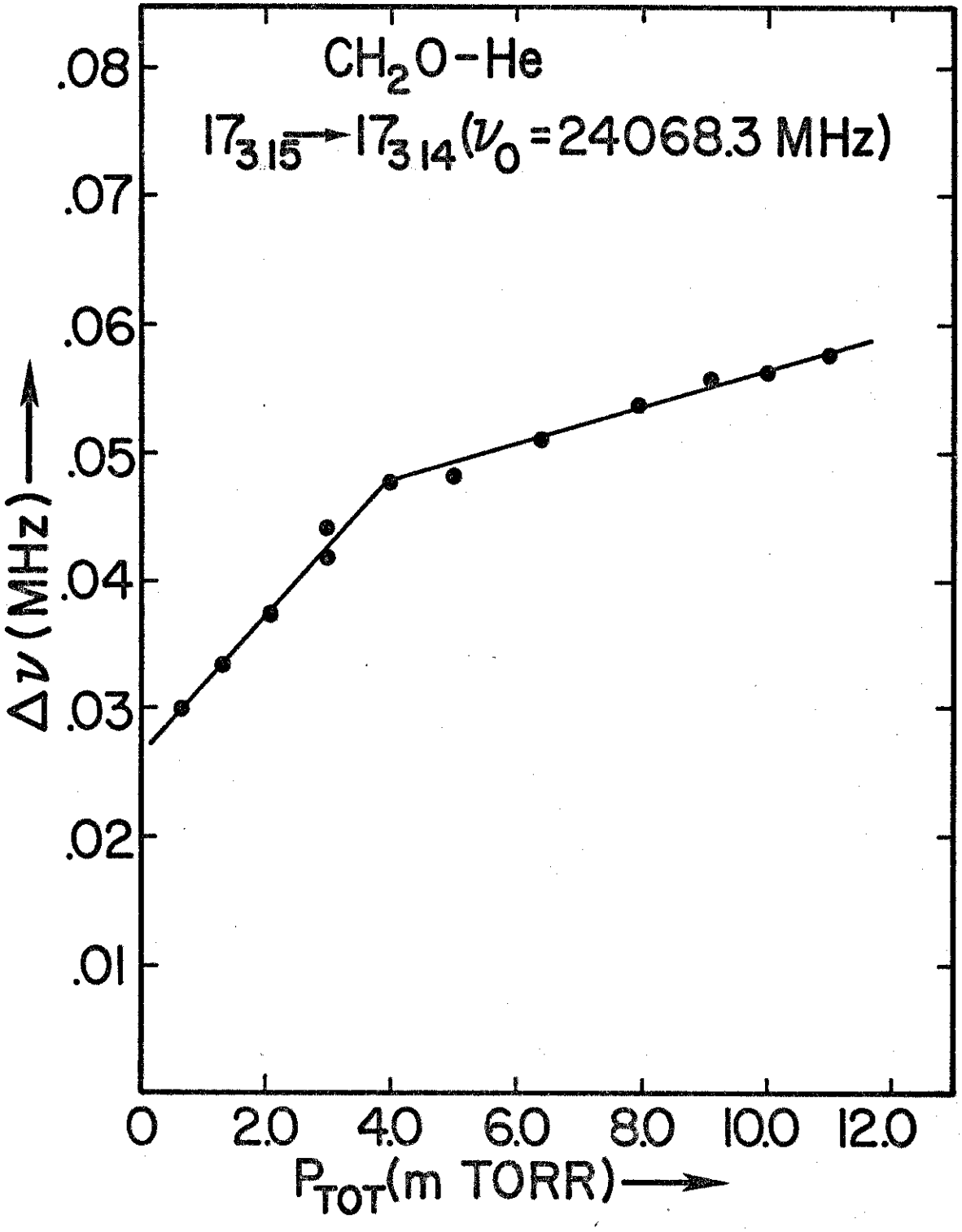

Fig. 19. Line width parameter curve for deducing collision diameters in CH_2O-He mixtures.

where b_1 and b_2 are the collision diameters for self and foreign-gas broadening respectively, α is the value of $\Delta\nu_p$ under conditions of self broadening, and β is the foreign-gas broadening parameter (due to H_2 or He). N_0 is Avogadro's number.

M_1 is the molecular mass of either HCOOH or CH_2O and M_2 is the "reduced" molecular mass of HCOOH (or CH_2O) and either of the foreign-gas molecules H_2 or He with a molecular mass M_f

$$1/M_2 = 1/M_1+1/M_f \ . \tag{47}$$

The measurements on the formic acid system indicate that for HCOOH-HCOOH interactions, there is a dependence of the line width parameters (and collision diameters) on the quantum number J (see Figure 20). The values for $\Delta\nu_p$ (and b_1) are approximately constant for $J \leq 12$, then decrease in the range $12 \leq J \leq 32$. The results of the line broadening parameter determinations for the foreign-gases did not yield a general trend in the values of $\Delta\nu_p$ as a function of J. However, the values of the collision diameters for H_2 and He seem to be approximately constant over the quantum number range $3 \leq J \leq 32$.

The behavior of the collision diameters at low pressures [i.e., the values labelled (a) in Table II] as a function of the quantum number J for the various interactions involving

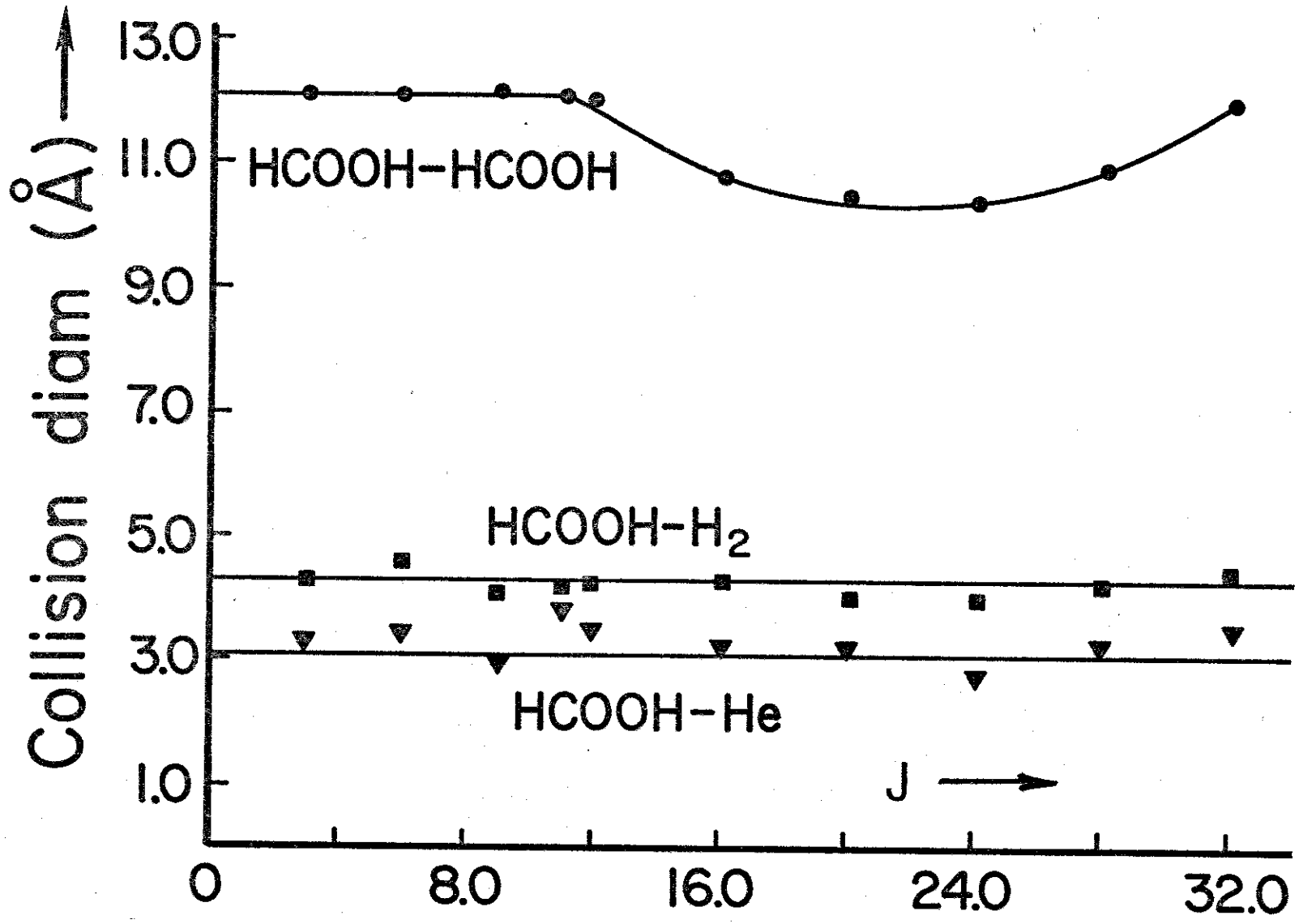

Fig. 20. Relative trend of the collision diameters for HCOOH rotational resonances for $3 \leq J \leq 32$.

the CH_2O molecule is shown in Figure 21. The microwave collision diameters were found to vary in magnitude from 11.70 − 15.90 Å for CH_2O-CH_2O interactions, 2.40 − 4.55 Å for CH_2O-He interactions, and 4.08 − 5.70 Å for CH_2O-H_2 interactions. The much stronger dependence of the various collision diameters on J (as compared to the collision diameters involving the HCOOH molecule) can generally be attributed to two causes. First, the larger dipole moment of the CH_2O molecule and second, the difference in energy spacings of the molecules. This dependence of the collision diameter on the dipole moment and energy spacings is examined later on in this chapter.

The physical interpretation given to collision diameters is that they measure the relative effectiveness of molecular collisions in broadening the various rotational energy levels by inducing transitions from a given level. For instance, CH_2O-He interactions are more effective in broadening the two levels involved in the transition $11_{2,10} \longrightarrow 11_{2,9}$ (with b_2=3.90 Å) than they are in broadening the two levels involved in the transition $25_{4,22} \longrightarrow 25_{4,21}$ (with b_2=2.40 Å).

In pressure broadening experiments two quantum levels (1 and 2) are specified as initial levels for the collision induced transitions and the broadening gives the sum of the probabilities of transitions from the two levels to all possible final levels, i.e., $\sum_f (\langle P_{1f} \rangle + \langle P_{2f} \rangle)/N$, where P_{if}

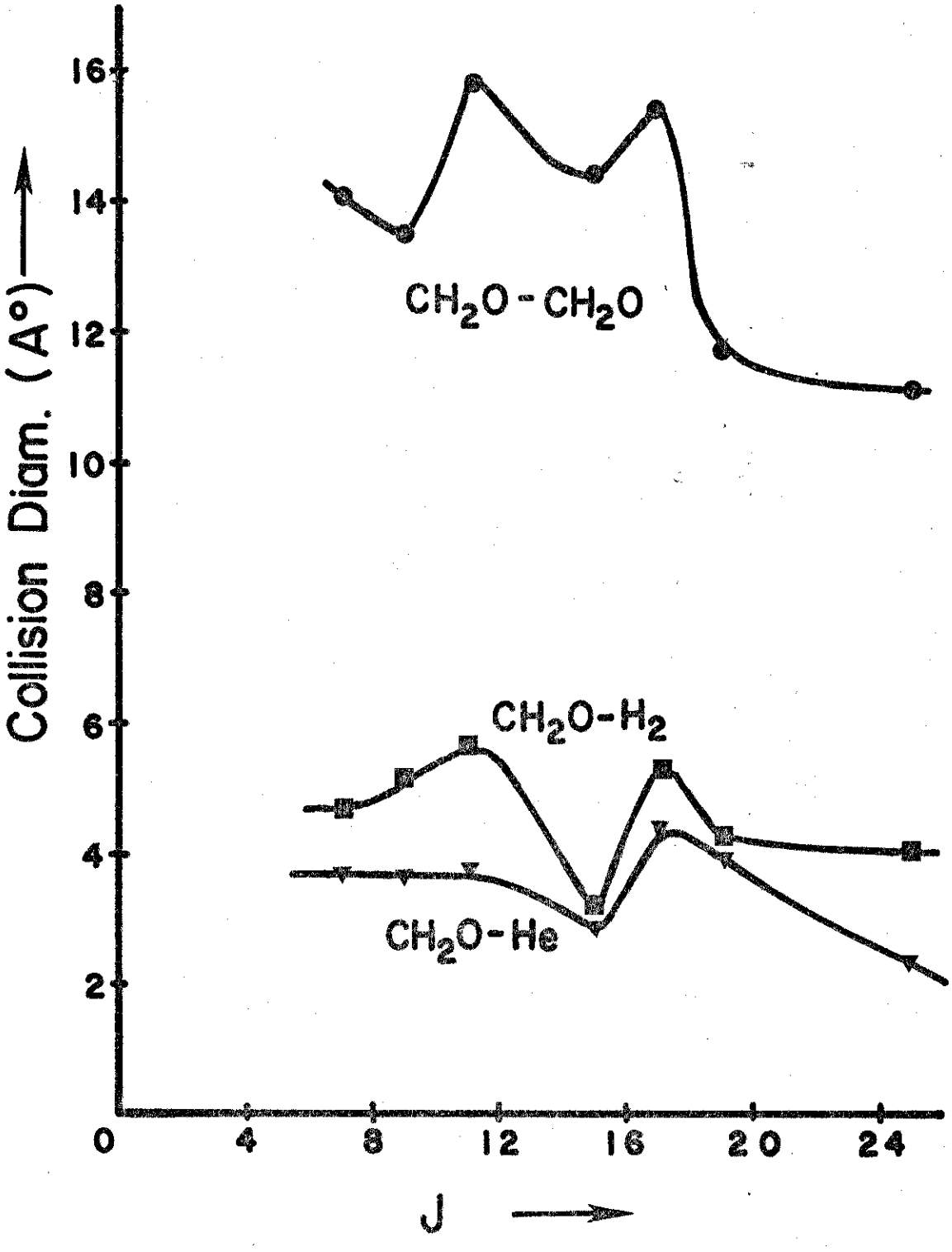

Fig. 21. Relative trend of the collision diameters for CH_2O rotational resonances for $7 \leq J \leq 25$.

is the probability of a collisionally-induced transition from an initial state i, and N the normalization factor. These measurements give the average time that a molecule stays in the particular rotational state 1 or 2, but do not give direct information on the selection rules, i.e., the relation between the initial and final levels. This is why the collision diameters are said to measure the relative effectiveness of collisional broadening; they don't serve to establish the absolute rate of collisionally-induced transitions between two particular states.

Error Estimate

Based on repeatability of measurements of the line width parameters, the values for $\Delta\nu_p$ are estimated to be in error by no more than ±5.0 per cent for measurements on the spectral lines of HCOOH, and ±7.0 per cent for CH_2O lines. These errors can be attributed to four main causes. First, some of the spectral lines were distorted by the presence of standing waves close to them. Whenever possible attempts were made to reduce the amplitude of these standing waves to a small value relative to the spectral line being observed. Complete elimination of this problem wasn't possible and hence the slight error in the value of $\Delta\nu$ was unavoidable. Second, the thermocouple gauge proved to be slightly non-linear in measuring pressure. Third, the repeatability of individual measurements of $\Delta\nu$ at a constant pressure suffered

occasionally from fluctuating klystron sweep rates, when the klystron could not "follow" the applied sawtooth with perfect consistency. Finally, a liberal error estimate should be chosen because many of the lines could not be corrected for overlapping hfs components, as the relative intensities and frequency splittings are unavailable.

Line Broadening Mechanisms

Murphy and Boggs[60] and Mehrotra and Boggs[67] have calculated theoretically the collision diameters for several self broadened CH_2O and HCOOH lines. The results of these calculations along with the corresponding experimental values are shown in Table III. All calculations were made assuming only dipole-dipole interactions. This assumption is valid since both molecules have permanent dipole moments and at low pressures the dipole-dipole interactions should predominate. From Table III, one notices that in general the theoretical values are greater than their experimental counterparts. The only exception being the $25_{4,22} \longrightarrow 25_{4,21}$ transition of CH_2O. The reason for the theoretical collisions diameters being larger than the experimental ones is not clear, since the dipole-dipole interactions used in these calculations are not the only intermolecular potentials present in these collisions, yet the calculated diameters

TABLE III

COMPARISON OF THEORETICAL AND EXPERIMENTAL COLLISION DIAMETERS FOR SELF-BROADENING INTERACTIONS OF HCOOH AND CH_2O

Molecule	Transition	Collision Diameter (Å)	
		Calculated	Experimental
HCOOH	$3_{1,3} \longrightarrow 3_{1,2}$	13.26	12.10
	$24_{4,21} \longrightarrow 24_{4,20}$	14.36	10.41
	$32_{5,28} \longrightarrow 32_{5,27}$	12.85	11.95
CH_2O	$9_{2,8} \longrightarrow 9_{2,7}$	18.20	13.51
	$17_{3,15} \longrightarrow 17_{3,14}$	15.77	15.48
	$25_{4,22} \longrightarrow 25_{4,21}$	11.30	12.13

are already too large. Any inclusions of higher order interactions like dipole-quadrupole, etc., interactions would further increase the values of the calculated collision diameters and produce even poorer agreement with the measured ones.

It should be noted that the discrepancies observed in Table III are not confined to the HCOOH and CH_2O systems; similar differences between theory (using Murphy-Boggs type calculations) and experiment are observed for most asymmetric top molecules.[60] There are two possible sources of errors that may account for this discrepancy. First, Murphy-Boggs type calculations tend to over-estimate the contributions from strong collisions, i.e., $b \leq b_0$ (see Figure 14), and underestimate the effects from more distant approaches, i.e., $b > b_0$. Due to the large dipole moments of CH_2O and HCOOH it is felt that more emphasis should be given to distant encounters (particularly at low pressures). Secondly, the disordered arrangement of the rotational energy levels of asymmetric top molecules[60] may "accidently" result in two levels being relatively close together and all other levels to which transitions can occur being far apart. This effect is important for light molecules or for high J transitions. Such an effect can lead to saturation of the K-doubled energy levels before transitions to other levels can occur. The spacings of energy levels should therefore be carefully examined before theoretical calculations on line broadening are attempted.

Despite the differences between the calculated and measured values for b_1, which range from approximately 2.0-27.0 per cent, it can be concluded that dipole-dipole interactions are primarily responsible for self-broadening of the rotational lines of HCOOH and CH_2O.

In establishing the likely mechanism for HCOOH-H_2 and CH_2O-H_2 broadening, the strongest interaction should be between the dipole moment of the absorber (either HCOOH or CH_2O) and the quadrupole moment of hydrogen (since diatomic hydrogen has no dipole moment). The quadrupole moment of H_2 is thought to be about 1.0 D-Å, but experimental determinations of the magnitude vary.[68] The quadrupole moments of formaldehyde and formic acid are not known, but there may be some quadrupole-quadrupole coupling also present in these interactions. In addition, there also exists the possibility of a weak dipole-induced dipole coupling. From Table IV, however, the dipole-quadrupole should be the dominant one with the other potentials contributing to a lesser extent.

On the other hand, for interactions of CH_2O (or HCOOH) with helium, the possible intermolecular potentials are rather limited since He has neither a dipole moment or a quadrupole moment. It is, however polarizable and has an isotropic polarizability[69] of $\alpha=2.06\times10^{-25}$ cm^3. Hence, the only possible interactions are of the type, dipole-induced dipole and quadrupole-induced dipole. From Table IV, the dipole-induced dipole potential should dominate in these

TABLE IV

IMPORTANT INTERMOLECULAR INTERACTIONS[a]

P	Multipole Interaction	Molecular Separation Dependence	C_p[b]
1	Dipole-dipole	R^{-3}	$\frac{4}{9}\left(\frac{\mu_1\mu_2}{\hbar v}\right)^2$
2	Dipole-quadrupole	R^{-4}	$\frac{16}{45}\left(\frac{\mu_1 Q_2}{\hbar v}\right)^2$
3	Quadrupole-quadrupole	R^{-5}	$\frac{16}{25}\left(\frac{Q_1 Q_2}{\hbar v}\right)^2$
4	Dipole-induced dipole	R^{-6}	$\frac{21\pi^2}{640}\left(\frac{\mu_1^2\alpha_2}{\hbar v}\right)^2$
5	Quadrupole-induced dipole	R^{-7}	$\frac{27\pi^2}{32}\left(\frac{\mu_1 Q_1\alpha_2}{\hbar v}\right)^2$

[a]Compiled from Ref. 4, p. 349.

[b]Notation: μ=dipole moment; Q=quadrupole moment; α=isotropic polarizability; v=mean relative velocity; and $\hbar=h/2\pi$.

collisions with some contribution from the quadrupole-induced dipole interactions.

To check the assumed foreign-gas broadening interactions in a rough fashion, approximations for the weighting factor $S_2(b)$ given in Equation (38) may be used to calculate the collision diameters for He and H_2 with the aid of Equation (39). Birnbaum[70] has shown that, for a symmetric top molecule perturbed by a linear molecule, the function $S_2(b)$ can be approximated in rather a simple form. Although HCOOH and CH_2O are asymmetric top molecules, they are both nearly prolate (asymmetry parameters of -0.95 and -0.96 respectively). Therefore, as a first approximation both molecules may be treated as prolate symmetric top molecules and Birnbaum's expressions should give some information as to the validity of the assumed interactions.

Starting with the interactions involving the hydrogen molecule, and taking the dipole-quadrupole potential as the dominant one, the expression for $S_2(b)$ is given by

$$S_2(b) = \frac{2C_2}{b^6} Q(J_2,K_2)\{1-K_1^2/(J_1+1)\} \quad . \tag{48}$$

The subscript 1 on the J,K quantum numbers refers to the absorber (either HCOOH or CH_2O) and subscript 2 refers to the perturbing molecule (He or H_2). Considering the $3_{1,3} \longrightarrow 3_{1,2}$ transition of HCOOH, and treating the HCOOH molecule

as a limiting prolate top, the appropriate quantum numbers are $J_1=3$ and $K_1=1$. Since H_2 is a linear molecule (i.e., $K_2=0$), Birnbaum has shown it is permissible to use the approximation $Q(J_2,0)\approx 1/4$. For the above transition, the quantity $S_2(b)$ reduces to

$$S_2(b) = \frac{0.47\ C_2}{b^6} \quad . \tag{49}$$

From the term for P=2 in Table IV, with $\mu=1.4$ D, $Q_2=1.0$ D-Å (the quadrupole moment of H_2), and $v=1.82\times10^5$ cm/sec (the relative velocity of HCOOH and H_2 at 300°K), one calculates $C_2=1893$ Å^6.

Since the interactions between HCOOH and H_2 are short range in nature, it is safe to apply the condition that $S_2(b_0)=1$, giving $b_0=3.12$ Å [from Equation (49)]. Using Equation (39) and the definition of b_e (effective collision diameter) gives

$$\pi b_e^2 = \pi b_0^2 + 2\pi 0.47\ C_2(1/4b_0^4) \quad . \tag{50}$$

Solving Equation (50) for b_e, using the values for b_0 and C_2 obtained above, yields the calculated value for the collision diameter $b_e=3.78$ Å. The corresponding experimental value for the collision diameter of H_2 for this transition (see Table I) is 4.31 Å. Although there is about 14.0 per cent difference between theory and experiment, the agreement

is rather good considering the approximate nature of the calculations. Similar calculations made on the other lines of HCOOH broadened by H_2 yield calculated values of the collision diameters to be in the range 3.70 – 3.83 Å. The almost constant value of the calculated collision diameters gives the correct trend for the variation of $b_2(H_2)$ with J (see Figure 22). The lower values obtained from theory suggest the strong possibility of some quadrupole-quadrupole etc., coupling also present in these interactions.

On the other hand, calculated values of $b_2(H_2)$ for CH_2O-H_2 interactions were found to be in the range 4.51 – 4.82 Å. The measured values of $b_2(H_2)$ are seen to be far more dependent on J (see Figure 21) than is revealed from Birnbaum's theory. It may be that for some of the high J lines of CH_2O other factors like the spacing of energy levels enter the picture. Nevertheless, these calculations do indicate that dipole-quadrupole interactions dominate in CH_2O-H_2 interactions with the possibility of higher order interactions also contributing.

In a similar fashion to that above, a check was made of the dipole-induced dipole coupling between HCOOH (or CH_2O) and He. An approximate expression of $S_2(b)$ for this interaction is given by[70]

$$S_2(b) = \frac{2\ C_5}{b^{10}} \{1 - Q_m(J_1, K_1)\} , \qquad (51)$$

where

$$Q_m(J_1,K_1) = \frac{3K_1^2 - J_1(J_1+1)}{(J_1+1)(2J_1+1)} \quad \frac{3K_1^2 - (J_1+1)(J_1+2)}{(J_1+1)(2J_1+3)} \quad . \qquad (52)$$

Considering the $3_{1,3} \longrightarrow 3_{1,2}$ transition of HCOOH, and treating the molecule as a limiting prolate symmetric top, the appropriate quantum numbers are $J_1=3$ and $K_1=1$. Substituting these quantum numbers in the definition of $Q_m(J_1,K_1)$ gives $Q_m(3,1)=0.152$, and so Equation (51) becomes

$$S_2(b) = \frac{2\ C_5}{b^{10}}\ (1-0.152) = \frac{1.72\ C_5}{b^{10}} \quad . \qquad (53)$$

From Table IV, C_5 is calculated using the quantities $\mu=1.4$ D, $\alpha=2.06\times10^{-25}$ cm, and $v=1.32\times10^{5}$ cm/sec (the mean relative velocity of HCOOH and He at 300°K). The value of C_5 is found to be 2660×10^{-80} cm^{10}.

Combining Equations (39) and (53) gives the expression for the effective collision diameter b_e

$$\pi b_e^2 = \pi b_0^2 + 2\pi(1.72\ C_5)(1/8\ b_0^8) \ , \qquad (54)$$

with b_0 being determined by the condition $S_2(b_0)=1$. Using the values of b_0 and C_5 thus obtained, the calculated value for $b_e=2.92$ Å. The corresponding experimental collision diameter of He for this transition (see Table I) is 3.34 Å. The agreement between theory and experiment is favorable.

Similar calculations made on the other rotational lines of HCOOH gave values for b_2(He) in the range 2.89-2.94 Å. Birnbaum's theory therefore correctly predicts the dependence of b_2(He) on J, except the calculated values are smaller than the measured ones, suggesting a strong possibility of contribution from quadrupole-induced dipole interactions in addition to the dominant dipole-induced dipole interactions.

In a similar fashion calculations were made for CH_2O-He interactions; this yielded values for $b_e(H_2)$ in the range 3.06 - 3.3 Å. As in the case of calculations made on the CH_2O-H_2 interactions, the above values for b_e do not show the dependency of the collision diameters on J (see Figure 21), again indicating that other factors (spacing of energy levels etc.) may be responsible for lack of better agreement between theory and experiment. The calculated values do indicate that dipole-induced dipole interactions are primarily responsible for the broadening with small contributions from other higher order interactions (e.g., quadrupole-induced dipole etc.).

Anomalous Behavior of CH_2O Lines

Pressure broadening experiments conducted on formaldehyde revealed that for a number of transitions, the line width parameter exhibited a curious behavior. It was observed that the slope of $\Delta\nu$ versus pressure undergoes an abrupt change as P becomes sufficiently high. A graph of $\Delta\nu$ vs.

p for one transition that exhibits this effect is seen in Figure 19. The line width parameter $\Delta\nu_p$, for the $17_{3,15} \longrightarrow 17_{3,14}$ transition of CH_2O broadened by He, is found to change its value from 5.37 MHz/Torr to 3.27 MHz/Torr at a pressure of about 4.0 mTorr. Examining Table II, one notes that this discontinuity in $\Delta\nu_p$ is more common for transitions involving high J values (i.e., $J \geq 15$); however, similar effects do exist for a few low J lines.[20] Except for the $15_{3,13} \longrightarrow 15_{3,12}$ and $17_{3,15} \longrightarrow 17_{3,14}$ transitions where this effect occurs for both self-broadening as well as for foreign-gas broadening in general, it is found that mostly self-broadened lines exhibit this behavior (see Table II).

The appearance of the "knee" in the plot of $\Delta\nu$ vs. p is seen to be pressure as well as temperature dependent for both foreign-gas broadening and self-broadening of CH_2O. In Figure 22, the line width parameter curve for self-broadening of the $17_{3,15} \longrightarrow 17_{3,14}$ line at various temperatures is shown. At room temperature ($T=300^{\circ}K$) the pressure at which the slope change occurs (P_B) is seen to be about 2.9 mTorr. As the temperature increases, the value of P_B increases correspondingly and at $T=309^{\circ}K$, $P_B=6.0$ mTorr. Furthermore, at any constant temperature it is found that the pressure required to produce the "knee" in the line width parameter curve is lower for self-broadening interactions than it is for foreign-gas interactions. This can be observed

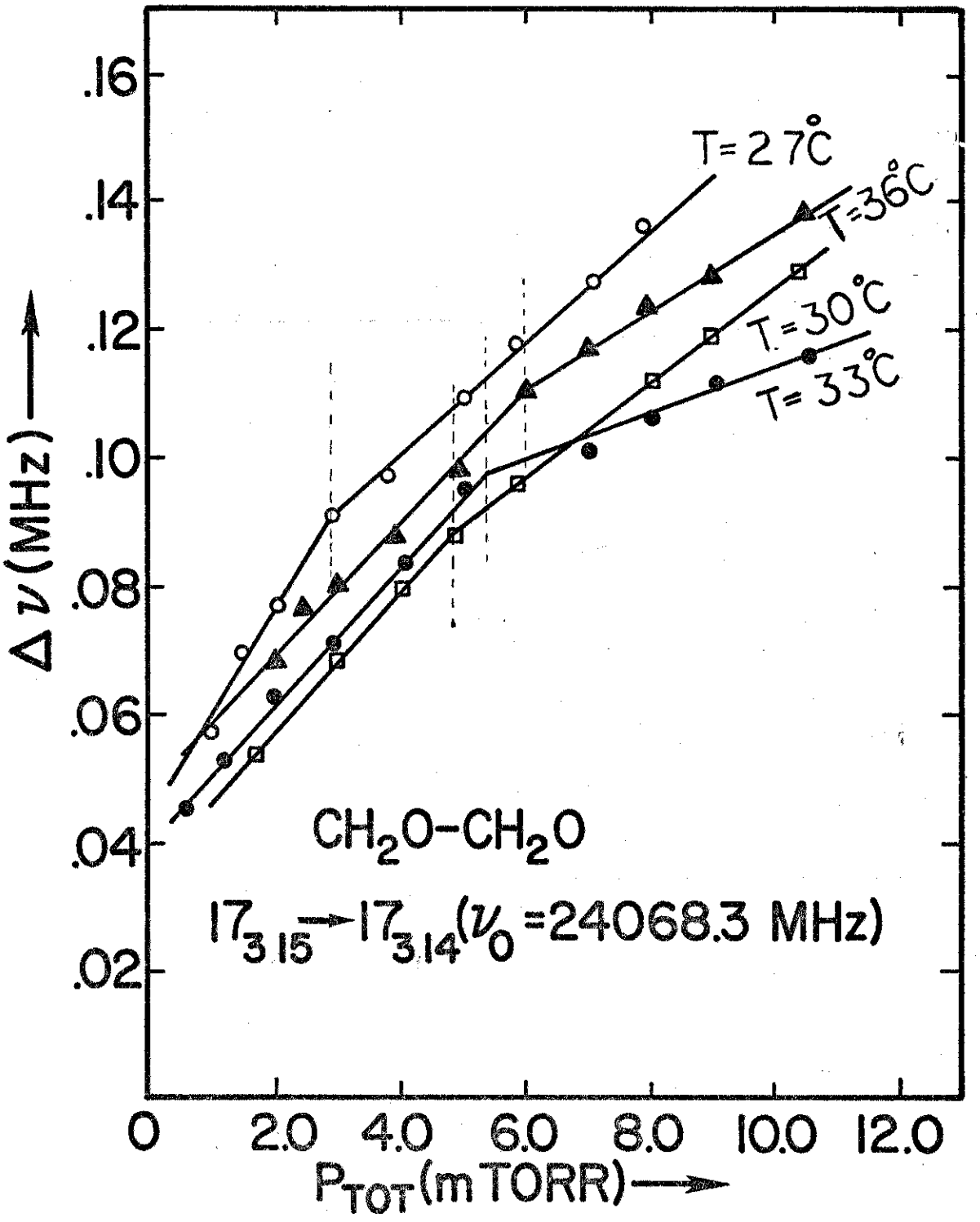

Fig. 22. Line width parameter curves at various temperatures for $17_{3,15} \longrightarrow 17_{3,14}$ transition of CH_2O.

from Figures 19, 22, and 23 where the values of P_B are found to be 4.0 mTorr, 2.9 mTorr, and 4.0 mTorr for CH_2O-He, CH_2O-CH_2O, and CH_2O-H_2 interactions respectively (for the $17_{3,15} \longrightarrow 17_{3,14}$ transition of formaldehyde at 300°K). Before an explanation for this "knee" effect can be given, the strong possibility of a number of causes which could be responsible for this abrupt change in $\Delta\nu_p$ has to be carefully examined.

External causes such as saturation and modulation effects can be discounted as extreme precautions were taken in these measurements (as discussed in Chapter III) to keep the power level of the radiation source (cause of saturation) and modulation voltage at low settings. In fact, to confirm the absence of any external effects on the system, the following analysis was conducted. Following measurements on the self-broadening of the $25_{4,22} \longrightarrow 25_{4,21}$ line of CH_2O (which was characterized by the "knee" effect), the gas in the cell (i.e., CH_2O) was pumped out and replaced by HCOOH vapor. Without changing any settings on the power level, modulation voltage,etc., pressure broadening experiments (both self and foreign-gas) were then carried out on a number of HCOOH lines. The results showed no discontinuity in $\Delta\nu_p$, indicating not only are external causes not responsible for the "knee" effect but that the latter is a real physical effect characteristic of the CH_2O molecule.

A second possible explanation for this effect could be attributed to the presence of hyperfine splitting observed

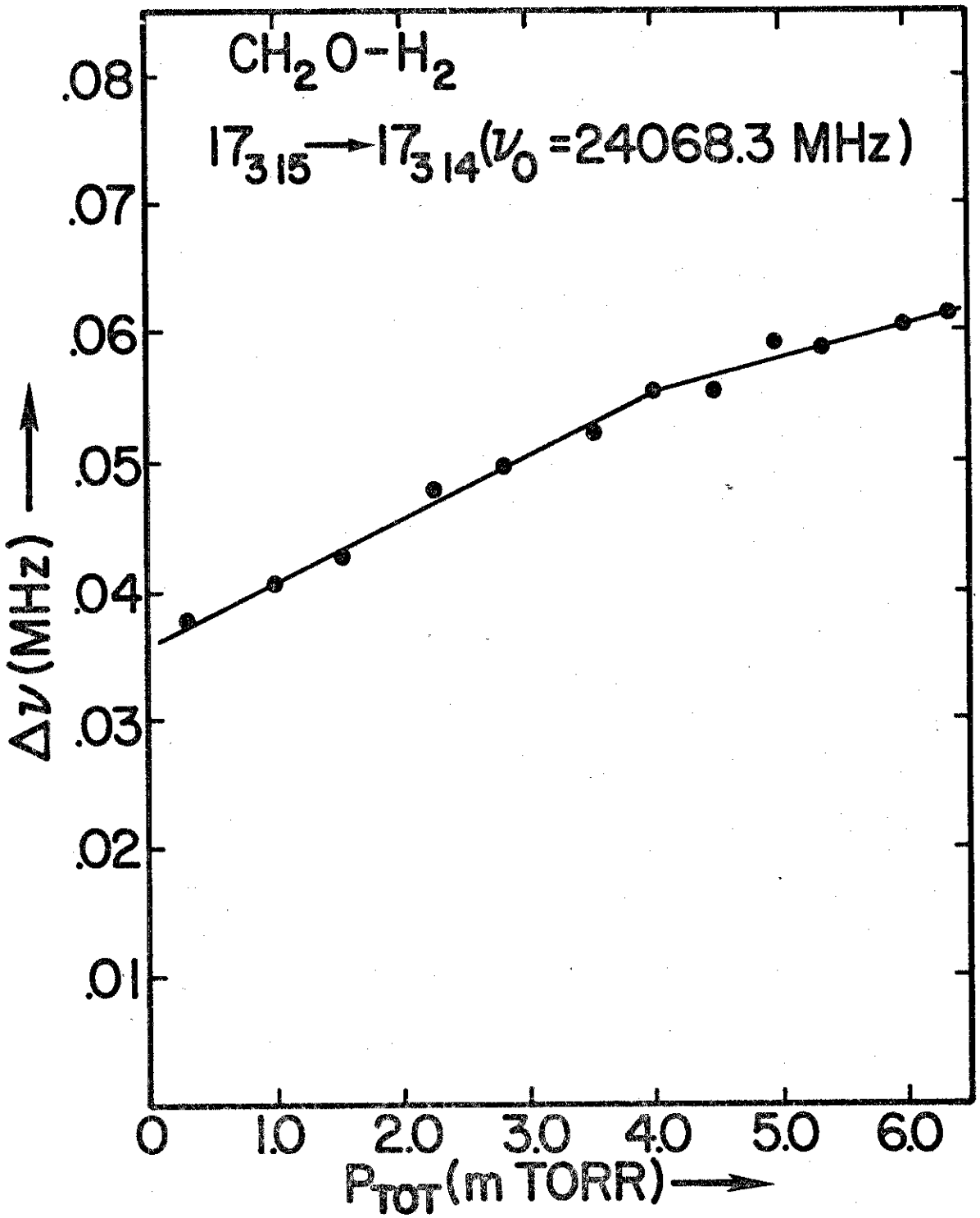

Fig. 23. Line width parameter curve for deducing collision diameters in CH_2O-H_2 mixtures.

in a number of CH_2O lines. However, it was found that for a number of lines where the splitting was as much as 20-30 KHz, no discontinuity in $\Delta\nu_p$ was observed. In addition, a theoretical model of overlapping Lorentzian shaped spectral lines failed to establish any relationship between hyperfine structure and the non-linear behavior of line width with changing pressure. One can therefore exclude hyperfine splitting in spectral lines as a possible cause of the "knee" effect.

The possibility of formaldehyde undergoing a chemical reaction (e.g., polymerization) or being absorbed (or desorbed) by the walls of the absorption cell has been considered. CH_2O does have a strong tendency to polymerize in the presence of such contaminants as water.[7] Assuming that a polymer of CH_2O is formed at a certain pressure, the broadening of CH_2O with the "new" gas may well be less, causing a decrease in the value of the line width parameter $\Delta\nu_p$. Such a molecule would have greatly different moments of inertia, hence, very different characteristic frequencies. Of course, this would still not explain the non-linearity in the line width plot in the case of foreign-gas broadening (Figures 19 and 23), as the partial pressure of formaldehyde was only a milli Torr or so, and remained constant throughout such measurements; however, if polymerization were to take place at a certain pressure, a gradual decrease in pressure would have to occur

as the gaseous phase was consumed into the polymer state. No such effect was observed; quite the contrary, the sample (i.e., CH_2O) appeared extremely stable and no polymerization was observed to occur even in the CH_2O reservoir, where CH_2O has remained for weeks at pressures much higher than that in the cell.

Similarly, if formaldehyde is being absorbed (or desorbed) by the cell walls, a gradual decrease (or increase) of the cell pressure would be detected. As already mentioned above no pressure fluctuations were observed throughout these measurements indicating the absence of such a phenomenon.

From the above discussion, it is evident that the discontinuity in $\Delta\nu_p$ is a real physical effect. A possible explanation for this effect can be arrived at by recognizing that the experimentally determined $\Delta\nu_p$ is actually a measure of the total collisionally induced transition rate from a given rotational energy level. An abrupt change in $\Delta\nu_p$ could indicate the strong possibility of a population-depopulation mechanism coming into existence at the critical pressure P_B.

In Figures 24 and 25, the natural log of the pressure at which the "knee" appears (i.e., P_B) have been plotted as a function of 1/T, where T is the temperature of the cell for the transitions $3_{1,3} \longrightarrow 3_{1,2}$ and $17_{3,15} \longrightarrow 17_{3,14}$ respectively. For the $3_{1,3} \longrightarrow 3_{1,2}$ transition, a positive slope

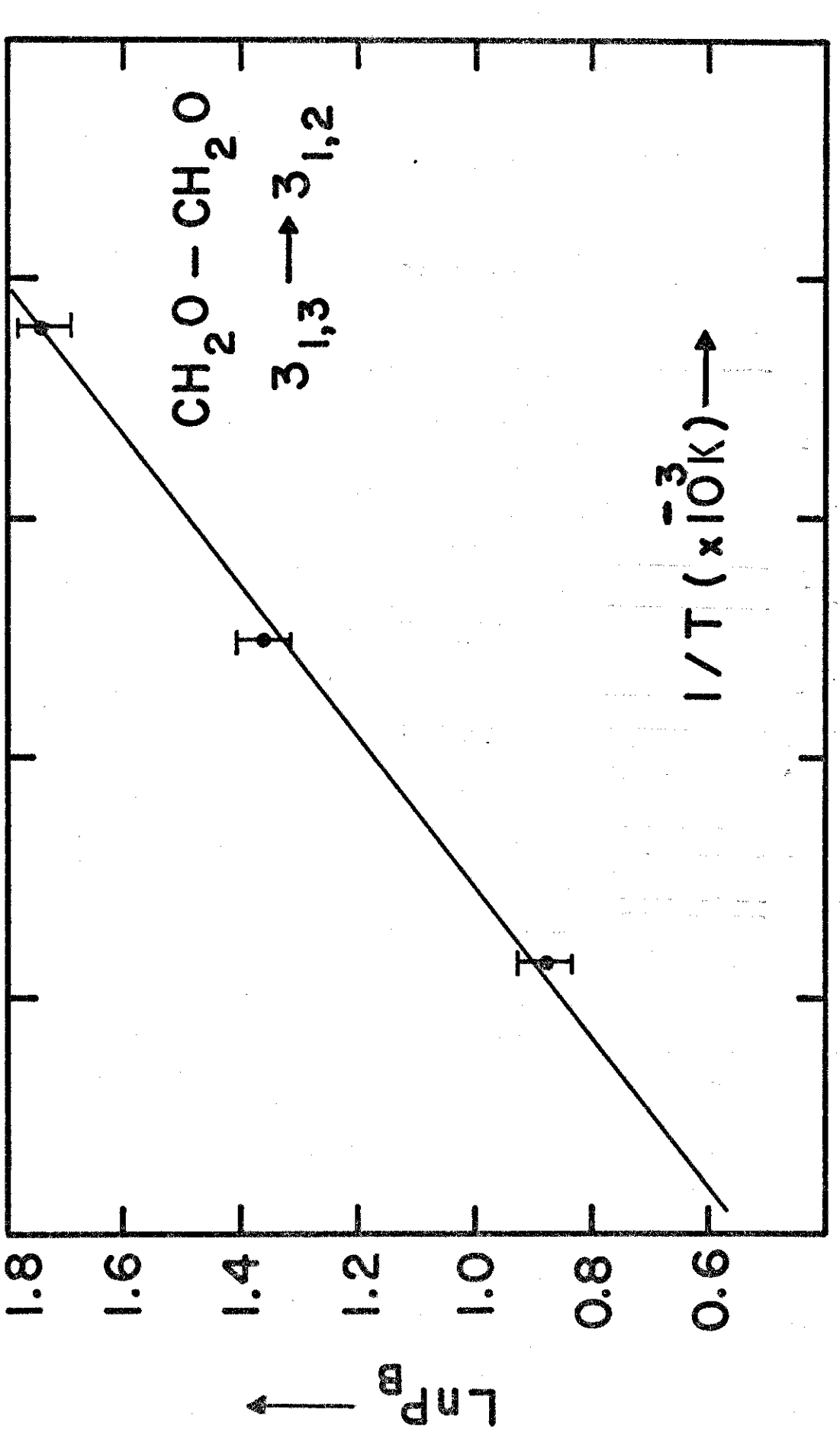

Fig. 24. Plot of Ln P_B vs. 1/T for the $3_{1,3} \longrightarrow 3_{1,2}$ transition of CH_2O.

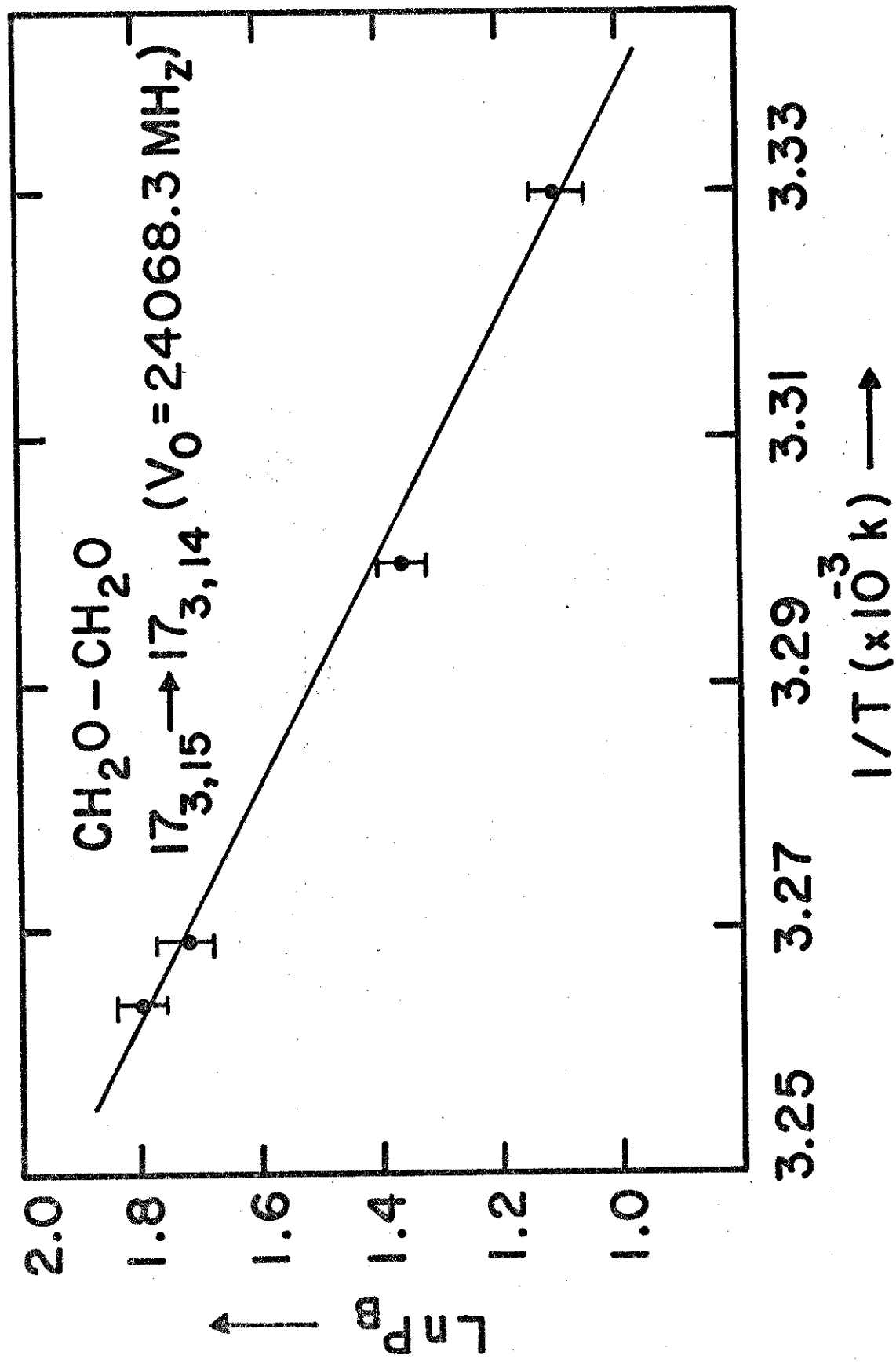

Fig. 25. Plot of Ln P_B vs. 1/T for the $17_{3,15} \longrightarrow 17_{3,14}$ transition of CH_2O.

was obtained indicating a possible decrease in the number of molecules being distributed amongst the "lower" rotational levels [since the cell pressure is proportional to n from Equation (31), and each rotational state has a fraction of these molecules distributed acording to Boltzmann statistics]. This effect can also be seen in Figure 26 where the line width parameter curves for the interaction CH_2O-CH_2O at various temperatures are displayed. For the $17_{3,15} \longrightarrow 17_{3,14}$ transition, the temperature study (Figure 25) shows a negative slope (for the plot of ln P_B vs 1/T) indicating a possible increase in the number of molecules being distributed amongst the "higher" rotational levels.

Molecular collisions are the main reason for the abrupt change in the value of $\Delta\nu_p$; however, there has to exist some other factor which makes this phenomenon unique to the CH_2O molecule. The logical candidate for this factor could be the relative spacing of the rotational energy levels. For example, if the spacing between the $16_{3,13}$ level and the $17_{3,15}$ level is such that collisions are capable of over populating the latter at the expense of the former, then one should expect the value of $\Delta\nu_p$ for the $16_{3,14} \longrightarrow 16_{3,13}$ transition to be less than that for the $17_{3,15} \longrightarrow 17_{3,14}$ line. The values of $\Delta\nu_p$ for the two above mentioned transitions (for self-broadening) are 20.0 MHz/Torr and 24.96 MHz/Torr respectively, indicating a strong possibility of one level

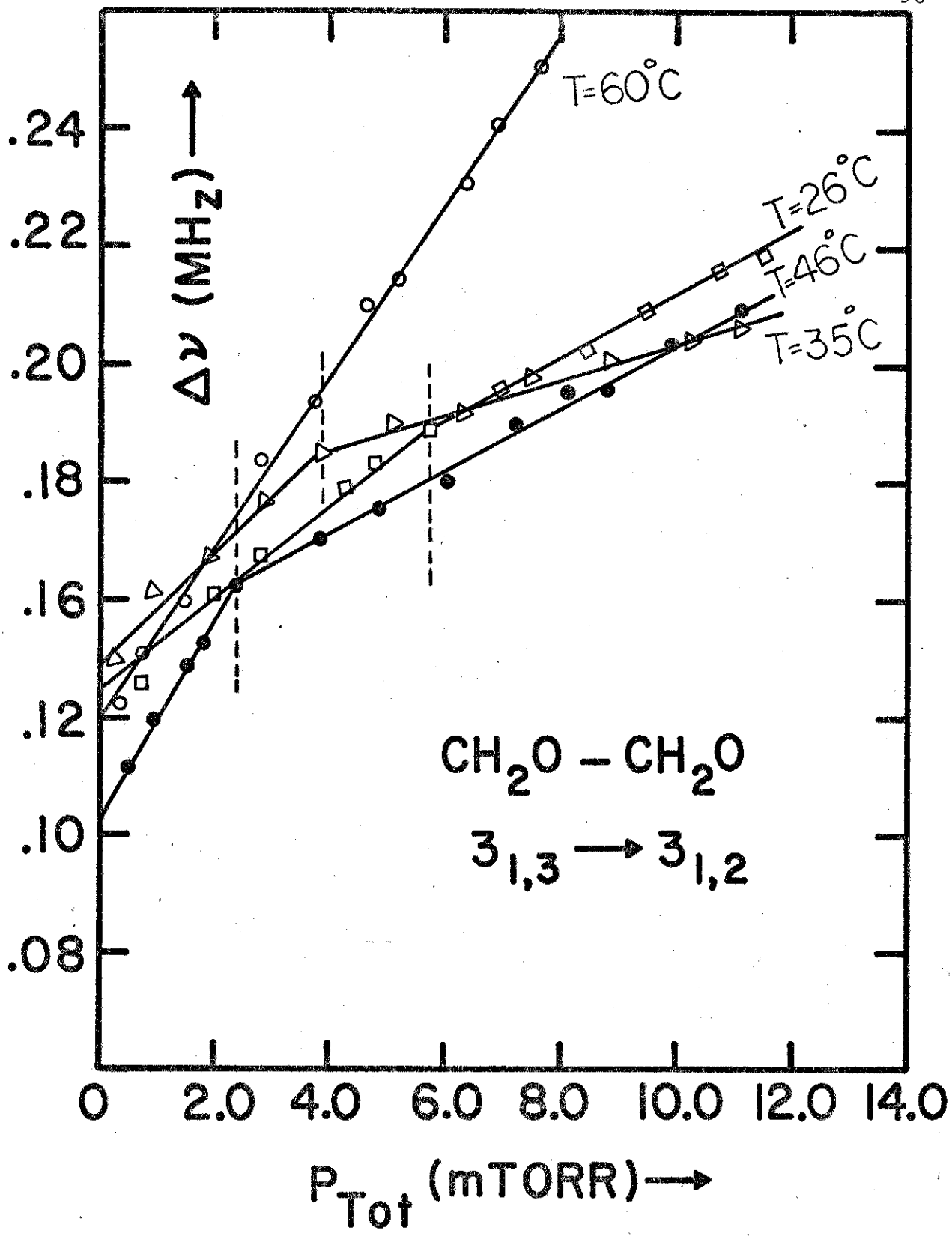

Fig. 26. Line width parameter curves at various temperatures for $3_{1,3} \longrightarrow 3_{1,2}$ transition of CH_2O.

being populated at the expense of the other. Similarly, the value of $\Delta\nu_p$ for the $3_{1,3} \longrightarrow 3_{1,2}$ transition is 14.5 MHz/Torr compared to 20.00 MHz/Torr for the $4_{1,4} \longrightarrow 4_{1,3}$ line, indicating the possibility of depopulation of the $3_{1,2}$ level at the expense of filling up the $4_{1,4}$ level.

In conclusion, it can be stated that the major objectives of this research problem have been realized in that precise measurements of microwave collision diameters, and an analysis of the inter-molecular forces responsible for broadening of the rotational lines of CH_2O and HCOOH have been successfully carried out. Furthermore, this investigation has revealed that the anomalous behavior of the line width parameter for several CH_2O transitions is a real physical effect which is strongly temperature and pressure dependent. Further investigation is, however, necessary to firmly establish the collisional pumping mechanism which is suspected to be the cause of this anomalous behavior. Such an investigation would require the separate monitoring of the population densities in the two or more rotational levels which are suspected to be involved in the population-depopulation effect. It is felt that application of "double resonance" techniques should shed more light on this problem. Such double resonance work is planned for the future in this laboratory, but it is not considered to be a part of this research problem.

APPENDIX

The rotational constants, asymmetry parameters, and the selection rules on the pseudo-quantum numbers K_{-1} and K_1 for the two asymmetric top molecules CH_2O and HCOOH are shown in Tables V and VI for the convenience of the reader.

TABLE V

ROTATIONAL CONSTANTS AND ASYMMETRY PARAMETERS FOR CH_2O AND HCOOH

Molecule	A (MHz)	B (MHz)	C (MHz)	κ
CH_2O	282029.00	38835.30	34003.20	-0.96
HCOOH	77512.25	12055.01	10416.20	-0.95

TABLE VI

ASYMMETRIC ROTOR SELECTION RULES FOR THE LIMITING PROLATE K

Component of $\vec{\mu}$	ΔK_{-1}
μ_a	$\pm 0, \pm 2, \pm 4, \ldots$
μ_b	$\pm 1, \pm 3, \pm 5, \ldots$
μ_c	$\pm 1, \pm 3, \pm 5, \ldots$

REFERENCES

1. C. E. Cleeton and N. H. Williams, Phys. Rev. 45, 234 (1934).

2. W. Gordy, W. V. Smith and R. F. Trambarulo, Microwave Spectroscopy (John Wiley and Sons, New York, 1953) p. 2.

3. W. E. Lamb and R. C. Retherford, Phys. Rev. 72, 241 (1947).

4. J. E. Wollrab, Rotational Spectra and Molecular Structure (Academic Press, New York, 1967) p. 29.

5. C. H. Townes and A. L. Schalow, Microwave Spectroscopy (McGraw-Hill, New York, 1955).

6. C. H. Townes and A. L. Schawlow, p. 342.

7. J. F. Walker, Formaldehyde (Reinhold, New York, 1964), 3rd ed., p. 37.

8. J. N. Schoolery and A. H. Sharbough, Phys. Rev. 82, 95L (1951).

9. H. Kim, R. Keller and W. D. Gwinn, J. Chem. Phys., 37, 2748 (1962).

10. R. Trombarulo, A. Clarck and C. Hearns, J. Chem. Phys., 28, 736 (1958).

11. L. E. Snyder, D. Buhl, B. Zukerman, and P. Palmer, Phys . Rev. Lett., 22, 679 (1969).

12. C. H. Townes and A. C. Cheung, Astrophys. J. 157, L103 (1969).

13. J. K. Bragg and A. H. Sharbough, Phys. Rev. 75, 1774 (1949).

14. R. B. Lawrence and M. P. W. Strandberg, Phys. 83, 363 (1951).

15. M. S. Cord, J. D. Peterson, M. S. Lojko, and R. H. Haas, Microwave Spectral Tables (NBS Monograph 70, Washington, D.C., 1968) Vol. IV, pp. 75-76.

16. R. B. Nerf, Jr., Astrophys. J. 174, 467 (1972).

17. G. S. Kukolich and D. J. Ruben, J. Mol. Spectrosc. 38 130 (1971).

18. A. Okaya, J. Phys. Soc. Japan 11, 249 (1956).

19. P. Palmer, B. Zuckerman, D. Buhl, and L. E. Snyder, Astrophys. J. 157, L 103 (1969).

20. D. V. Rogers and J. A. Roberts, J. Mol. Spectrosc. 46, 200 (1973).

21. J. D. Rogers and D. Williams, Phys. Rev. 83, 210 (1953).

22. R. G. Lerner, B. P. Dailey and J. P. Friend, J. Chem. Phys. 26, 680 (1957).

23. J. Bellet, C. Samson, and R. Wertheimer, C. R. Acad. Sc. Paris, t. 262, Serie B - 1333 (Mai 1966).

24. B. Zuckerman, J. A. Ball, and C. A. Gottlieb, Astrophys. J. 163, L41 (1971).

25. R. P. Netterfield, R. W. Parsons, and J. A. Roberts, J. Phys. B5, 146 (1972).

26. H. A. Lorentz, The Theory of Electrons (Dover, New York, 1909), note 57.

27. J. H. Van Vleck and V. F. Weiskoff, Rev. Mod. Phys. 17, 227 (1945).

28. Townes and Schalow, p. 343.

29. W. Heitler, The Quantum Theory of Radiation (Oxford University Press, London).

30. Townes and Schawlow, p. 342.

31. Townes and Schawlow, p. 336.

32. A. Beiser, Concepts of Modern Physics (McGraw Hill: New York, 1967), Rev. ed. p. 45.

33. R. W. Parsons and J. A. Roberts, J. Mol. Spectrosc. 18, 412 (1965).

34. B. Carnahan. H. A. Luther, and J. O. Wilkes, Applied Numerical Methods (J. Wiley, New York, 1969) p. 264.

35. M. Abramowitz and I. A. Stegun, Handbook of Mathematical Functions (NBS, Washington, D. C., 1964), p. 924.

36. M. Danos and S. Geschwind, Phys. Rev. 91, 1159 (1953).

37. W. Gordy, Microwave Spectroscopy, Rev. Mod. Phys. 20, 668-717 (1948).

38. C. H. Townes, Phys. Rev. 70, 665 (1946).

39. B. Bleaney and R. P. Penrose, Phys. Rev. 70, 775 (1946).

40. T. A. Pond and W. F. Cannon, Phys. Rev. 72, 1121 (1947).

41. R. L. Carter and W. V. Smith, Phys. Rev. 73, 1053 (1948).

42. R. Karplus and J. Schwinger, Phys. Rev. 73, 1020 (1948).

43. R. Karplus, Phys. Rev. 73, 1027 (1948).

44. E. A. Reinhart, R. H. Kleen, and C. C. Lin, J. Mol. Spectrosc. 5, 458 (1960).

45. D. V. Rogers, unpublished Ph.D. dissertation, North Texas State University (1972).

46. Townes and Schawlow, p.194.

47. A. Okaya, J. Phys. Soc. Japan 11, 258 (1956).

48. H. Takuma, T. Shimizu, and K. Shimoda, J. Phys. Soc. Japan 14, 1595 (1959).

49. P. Thaddeus, L. C. Krisher, and J. H. N. Loubser, J. Chem. Phys. 40, 257 (1964).

50. H. Kuhn and F. London, Phil. Mag., 18, 983 (1934).

51. H. Margenau, Phys. Rev. 82, 156 (1951).

52. Townes and Schawlow, p. 353.

53. P. W. Anderson, PHys. Rev. 76, 647 (1949).

54. J. S. Murphy and J. E. Boggs, J. Chem. Phys. 47, 691 (1967).

55. C. J. Tsao and B. Curnutte, J. Quant. Spectrosc. Radiat. Transfer 2, 41 (1962).

56. R. P. Futrelle, Phys. Rev. A 5, 2162 (1972).

57. J. S. Murphy and J. E. Boggs, J. Chem. Phys. 47, 4152 (1967).

58. _____, J. Chem. Phys. 49, 3333 (1968).

59. _____, J. Chem. Phys. 50, 3320 (1969).

60. _____, J. Chem. Phys. 51, 3891 (1969).

61. Townes and Schawlow, p. 356.

62. I. C. Story, V. I. Metchnik, and R. W. Parsons, J. Phys. B 4, 593 (1971).

63. G. Birnbaum, Intermolecular Forces (Interscience, New York, 1967), ed. by J. O. Hirshfelder, Chap. 9.

64. J. A. Roberts, Rev. Sci. Instr. 45, 935 (1969).

65. Townes and Schawlow, pp. 407-408.

66. J. H. Jeans, Dynamical Theory of Gases (Cambridge Univ. Press, New York, 1921), 3rd ed., pp. 37, 252.

67. S. C. Mehrotra and J. E. Boggs, Univ. of Texas (Austin), private communications.

68. Krishnaji and V. Prakash, Rev. Mod. Phys. 38, 690 (1966).

69. R. W. Parsons, V. I. Metchnik, and I. C. Story, J. Phys. B 5, 1221 (1972).

70. G. Birnbaum, J. Chem. Phys. 42, 2455 (1967).

71. P. Cross, R. M. Hainer, and G. W. King, J. Chem. Phys. 12, 210 (1944).